

NOTICE

**CERTAIN DATA
CONTAINED IN THIS
DOCUMENT MAY BE
DIFFICULT TO READ
IN MICROFICHE
PRODUCTS.**

LBL--29762

DE91 005325

Monte Carlo Calculation of "*Skyshine*"
Neutron DOSE from ALS

Mehrdad Moin-Vasiri
M.S. Thesis

College of Engineering
University of California

and

Accelerator and Fusion Research Division
Lawrence Berkeley Laboratory
University of California
Berkeley, CA 94720

June 1990

DISCLAIMER

This report was prepared as an account of work sponsored by an agency of the United States Government. Neither the United States Government nor any agency thereof, nor any of their employees, makes any warranty, express or implied, or assumes any legal liability or responsibility for the accuracy, completeness, or usefulness of any information, apparatus, product, or process disclosed, or represents that its use would not infringe privately owned rights. Reference herein to any specific commercial product, process, or service by trade name, trademark, manufacturer, or otherwise does not necessarily constitute or imply its endorsement, recommendation, or favoring by the United States Government or any agency thereof. The views and opinions of authors expressed herein do not necessarily state or reflect those of the United States Government or any agency thereof.

This work was supported by the U.S. Department of Energy under
Contract No. DE-AC03-76SF00098.

MASTER

DISTRIBUTION OF THIS DOCUMENT IS UNLIMITED

TABLE OF CONTENTS

Title	Page
1.0 INTRODUCTION.....	1
1.1 Radiation from the ALS.....	1
2.0 Sources of radiation.....	3
2.1 Synchrotron Radiation.....	3
2.2 Bremsstrahlung Radiation.....	5
2.3 Giant Resonance.....	8
2.3.1 Skyshine Radiation.....	8
2.3.2 Skyshine Radiation for accelerators.....	9
2.4 High Energy Neutrons.....	10
3.0 ALS Modeling for skyshine calculations.....	12
3.1 Modeling the source and shielding geometry.....	12
3.2 Modeling Source Strength for the Storage Ring.....	12
4.0 MORSE MONTE-CARLO.....	16
4.1 Description of MORSE CODE.....	16
4.1.1 Boundary Crossing Estimators.....	17
4.1.2 Point-Detector Estimators.....	17
4.3 Cross-Section sets.....	19
4.4 Conversion of spectra to Dose Equivalent.....	20
4.5 MORSE shielding Geometry.....	21
4.6 MORSE detector geometry for Storage Ring.....	22
5.0 IMPLEMENTATION OF MORSE.....	26
5.1 Commissioning Tests with Vacuum and Air.....	26
5.2 First results with air and concrete.....	27
6.0 Results of skyshine calculations from Storage Ring.....	28
6.1 neutron fluence and dose-equivalent no roof(radial).....	28
6.2 neutron fluence and dose-equivalent no roof(altitude).....	28
6.3 Neutron Spectra with no roof.....	30
6.4 Neutron dose and fluence with roof(radial).....	31
6.5 dose and fluence with roof (altitude).....	33
7.0 Comparison of MORSE shielding calculations.....	
with analytical models.....	35
7.1 Shielding Calculations.....	35
7.1.1 MORSE in shielding.....	36
7.1.2 Comparison of analytical calculations with MORSE.....	36
7.2 Comparison of an approximate skyshine.....	
calculation with MORSE.....	36
8.0 Summary and Conclusions.....	38
9.0 References.....	40

Title	page
A. Appendices.....	42
A1.0 MORSE structure.....	42
A1.1 Routines.....	43
A1.1.1 Main Routine.....	43
A1.1.2 Physical analogies corresponding to MORSE weight.....	44
A1.1.3 MORSE (NFLT).....	45
A1.1.4 Subroutine BANKR (NBNKID).....	46
A1.1.5 Subroutine SOURCE.....	47
A1.2 Input data.....	49
A1.2.1 Input data file (for ALS).....	49
A1.2.2 Geometry.....	55
A1.2.3 Fluence to dose conversion by ICRP factors.....	60
A2.0 Total power radiated.....	63
A3.0 Bremsstrahlung.....	64
A4.0 Sources of radiation for shielding calculations.....	66

ACKNOWLEDGEMENT

I would like to dedicate this work to two special people; on my father, from whose inspiration I reached this point of excellence in my life. He lost his battle to evil in IRAN in 1986. And to Dr. William Swanson without whom this work would have been impossible. He gave me encouragement, and unselfishly shared his great knowledge with me. He also lost his battle to cancer in 1988.

I also like to thank, my great advisor professor S. Kaplan who did not deny me of any thing from his personal time and effort to providing funding for a portion of this work.

My special thanks to Dr. Ted Jenkins at SLAC, who spent many hours to educate us about MORSE, and Mr. Ed Sheena at LBL whose computer knowledge made a great contribution to this work. I like to thank the other two member of my committee, professors Grossman and Prussin for their help to improve this work further.

And finally my thanks to all the wonderful people of Environmental Health and Safety at LBL who made my experience of working with them so pleasant.

Berkeley, California

June, 1990

1.0 INTRODUCTION

1.1 Radiation from the ALS

Light is a fundamental tool of science. Optical microscopy, astronomy, the spectroscopies of the physicist and chemist all depend on it. For more than two decades lasers have been the dominant source in the visible and infrared regions of the electromagnetic spectrum. The most powerful sources of X-rays and ultraviolet radiation are particle accelerators, where circulating electrons emit light as a by-product of their motion.

The Advanced Light Source (ALS) was designed specifically to provide intense beams of light in the electromagnetic spectrum between 10 to 5000 eV. Electrons forced to follow a curved trajectory emit light (so-called *synchrotron radiation*) whose characteristics depend on the energy of the electrons and the radius of the curved path. In the Electron Storage Ring of the ALS, electrons circulate for many hours at a constant energy, variable between 1 and 1.9 GeV , constrained by magnets to nearly circular orbits. Electrons constrained in such orbits emit sweeping beams of light. In addition, for experimental use the light can be enhanced and delivered by means of alternating magnetic field strips called undulators and wigglers. A typical beamline comprises mirrors and other optical components whose purpose is to guide the synchrotron radiation from its source (the electron beamline in the storage ring) to an experimental station. Undulators and wigglers are inserted in the straight sections of the electron storage ring. These magnetic structures are called insertion devices, and they tend to bend the electrons back and forth along a straight path. Ultimately, the ALS will include eleven insertion devices with both the undulators and wigglers and provisions for up to 60 beamlines for transporting the light to experimental areas.

The electron-beam acceleration and transport in the ALS consists of three sections(Figure 1.1), the linear accelerator (LINAC) with an energy of 50 MeV, the booster ring with the energy of 1 GeV, and the storage ring with a constant energy variable between 1

and 1.9 GeV. Once accelerated by the linear accelerator and small booster synchrotron, the electrons are injected into the storage ring, where they circulate for up to 3 hours at constant energy (variable between 1- 1.9 GeV).

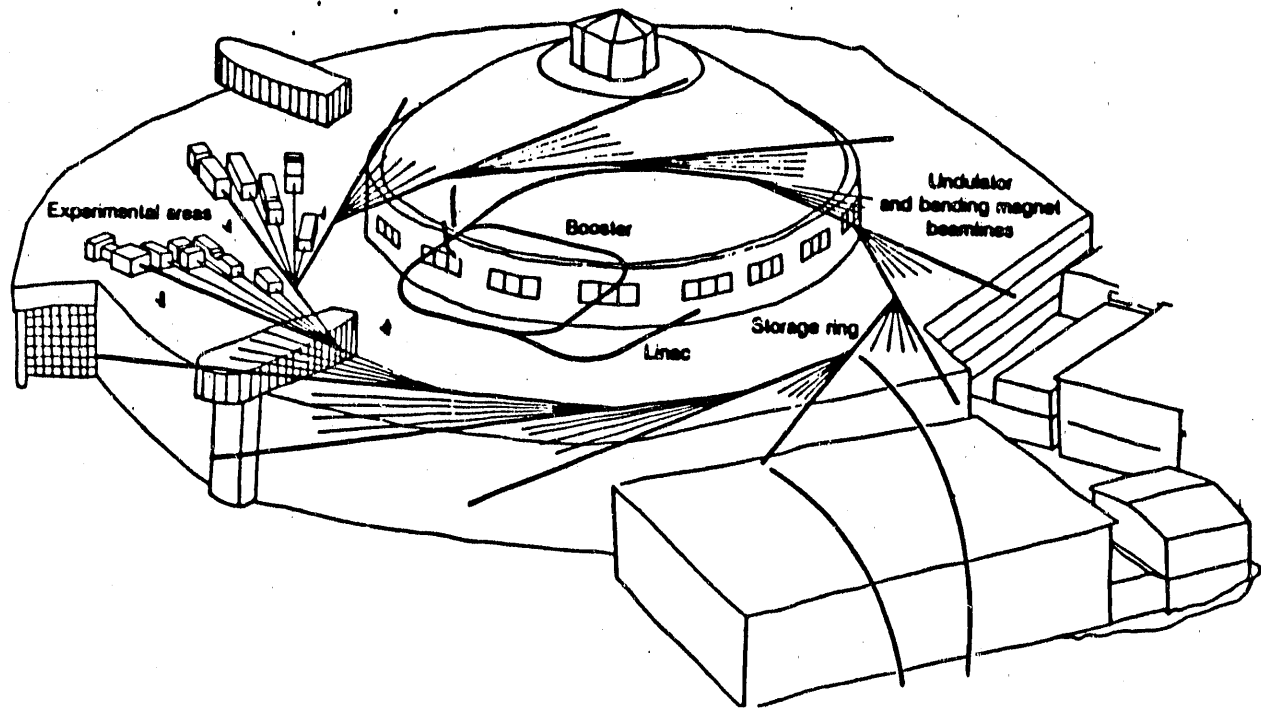


Figure 1.1, Linac, Booster, and Storage Ring of the Advance Light Source facility. The beam line comprises mirror and other optical components to quid synchrotron radiation from its source.

2.0 Sources of radiation

In the energy range at which most electron storage rings operate (from hundred MeV to few GeV), there are many sources of radiation. First, *synchrotron radiation* which is the primary source of radiation transported to experimental areas. Synchrotron radiation does not impose a potential radiation hazard. The potentially harmful radiation is caused by two sources: *high-energy bremsstrahlung*, which is produced when the circulating beam is lost from orbit, and *giant resonance* photoneutrons produced in the resulting radiation shower. Another source of hazardous radiation is the production of *high energy neutrons* at 1.1 GeV range. All these radiation types are discussed below.

2.1 synchrotron radiation

Whenever relativistic electrons are bent in a magnetic field, a continuous spectrum of electromagnetic radiation known as *synchrotron radiation* is emitted. The frequency spectrum of the *synchrotron radiation* is given by equation 1 (ref. 13) and figure 2.1(ref. 13)

$$I(\omega) = 2\sqrt{3} \frac{e^2}{c} \gamma \frac{\omega}{\omega_c} \int K(x)_{5/3} dx \quad (2.1)$$

where the ω_c is the critical frequency,

$$\omega_c = 3 \left(\frac{E}{mc^2} \right)^3 \frac{c}{R_m} \quad (2.2)$$

and $K(x)_{5/3}$ is the modified Bessel function of order 5/3 (Ref. 13).

In the ALS the beam orbit consists of alternating straight and bending section. It therefore has an effective orbital radius, R , and a smaller magnetic radius R_m . The power radiated by an electron in such an orbit is given by:

$$P = \frac{2}{3} \frac{e^2}{RR_m} c \beta^4 \gamma^4 * \quad (2.3)$$

* appendix A2.0.

$$\text{where } \gamma = \frac{E}{0.511}.$$

For the ALS, $R = 30 \text{ m}$, $R_m = 4.874 \text{ m}$.

The synchrotron photon energy corresponding to the critical frequency ω_c is equal to (Ref.13):

$$E_c = \hbar \times \omega_c \quad (2.4)$$

At the maximum beam energy, $E=1.9 \text{ GeV}$ (for conservative shielding purposes, The maximum beam energy of 1.9 Gev, and twice the presently planned operating current of 0.4 A is used), this corresponds to $E_c = 6.24 \text{ KeV}$. This does not, therefore, constitute a significant shielding problem. The radiated power is given in table 1.

Additional synchrotron radiation from undulators and wigglers amounts to 5.6 Kw, and because of the low energy range this additional radiation is also not an important source of radiation in shielding design.

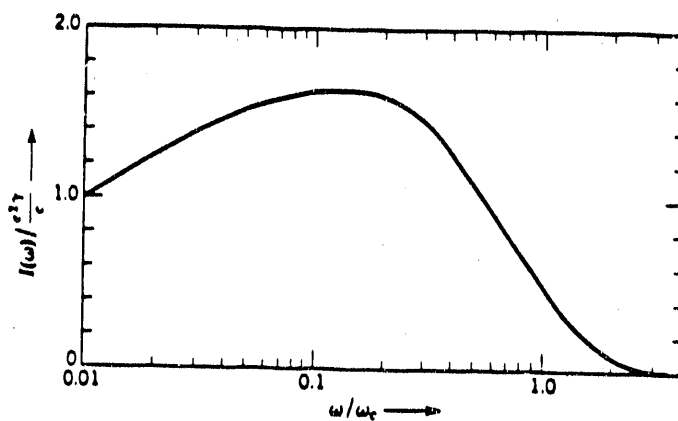


Figure 2.1, Synchrotron radiation spectrum as a function of frequency.

Table 1. synchrotron Radiation power Based on Maximum energy of 1.90 GeV, and 0.8 A.

	per circulating electron.	total
BEAM ENERGY	1.90 Gev	1000 Joules
ENERGY RADIATED PER CYCLE	0.238 MeV/ e^-	0.125 J
POWER RADIATED per particle	3.8×10^5 MeV/sec	200 KW
WIGGLERS AND UNDULATORS		5.6 KW

• 2.2 Bremsstrahlung Radiation

As circulating beam is lost from orbit it interacts in the vacuum walls of the accelerator ring. The high-energy electrons are decelerated by electric fields of the target nuclei resulting in the radiation of photons of energies ranging from 0 to E, where E is the electron energy. This mechanism is known as *Bremsstrahlung*. At high energies, the interaction of the generated photons with other target nuclei causes the electron pair production. The succession of bremsstrahlung and pair production is known as an *electromagnetic cascade or shower*. The distance which an electron travels for its energy to drop by a factor of 1/e, is called the *radiation length*.

The development of the shower depends on the thickness of the target. The radiation first increases with increasing target thickness until it reaches a maximum. Then, because of energy absorption, it declines exponentially. The average bremsstrahlung dose can be predicted with sufficient accuracy that normal shielding requirements can be determined. The bremsstrahlung radiation can be calculated by the following equation (Ref. 18):

$$D = (6 \times 10^4 E 2^{-\frac{\theta}{\theta_{1/2}}} + 3 \times 10^6 \times 10^{-\frac{\theta}{21}} + 9 \times 10^4 \times 10^{-\frac{\theta}{110}}) \frac{1}{3.6 \times 10^6} * \quad (2.5)$$

where

D is dose at 1 m from the electron-ring in $\text{rad} \cdot \text{m}^2/\text{J}$.

E is electron-ring energy in MeV.

θ is angle of radiation, with respect to the beam direction in degree.

$$\theta_{1/2} = \frac{100}{E} \text{ degree.}$$

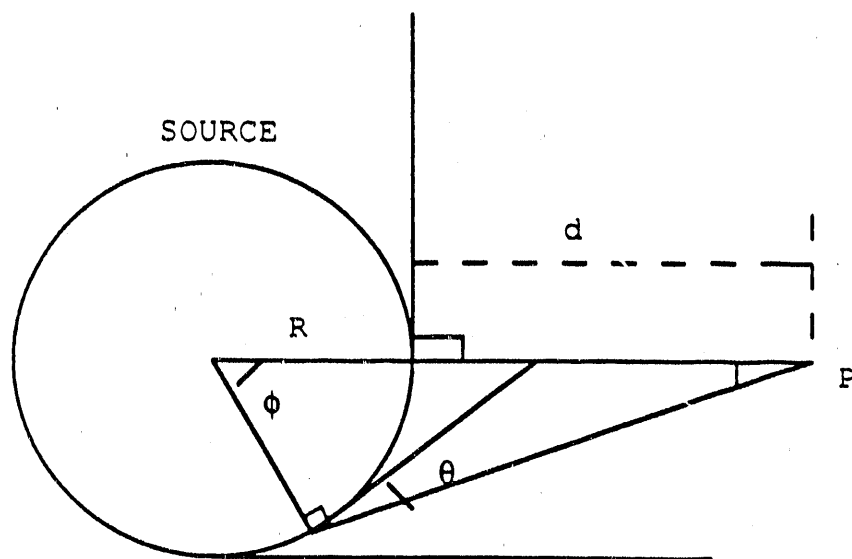


Figure A.5, Geometry for bremsstrahlung dose calculations at point P. A distance d from the beam.

Figure 2.2 shows the unshielded bremsstrahlung dose in the plane of the ring as a function of distance from the ring source as a function of radial distance from the ring.

These curves were obtained by numerical integration along the ring source, assuming a uniform beam loss. The circumference was divided into 199 segments (100 equal width segments over a 3.6° arc centered at $\theta = 0$, and 99 equal segments over the remainder of the circumference) and the dose increment along the X-axis, was found by computing angle θ from -30.0 to 200.0 meter (the source is at 0.0 m). The dose at -30 m indicates the dose at ring center which has $\theta = 90^\circ$ for every segment. The dose outside of the ring is more than the dose inside the ring at the same distance because of the forward peaking of the bremsstrahlung. The results are consistent with reference 18.

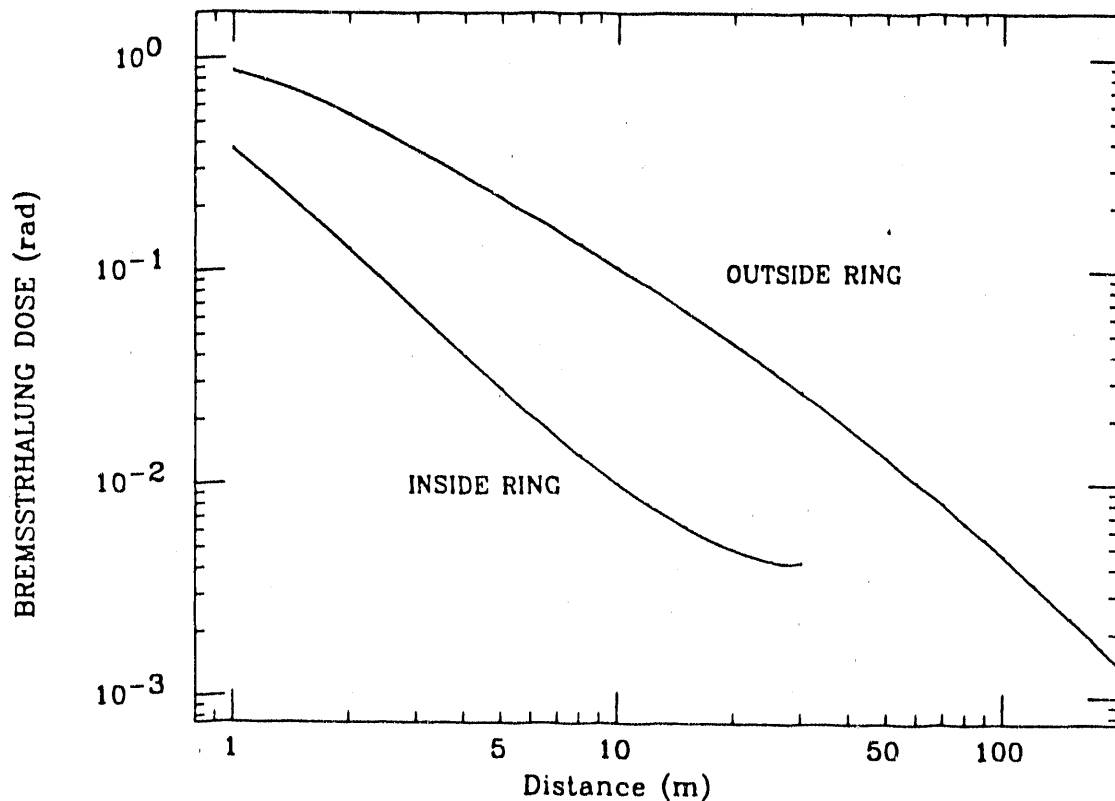


Figure 2.2, Bremsstrahlung dose inside and outside of the Storage Ring vs. distance for a 1.9 GeV beam at a radius of 30 meters.

- **2.3 Giant Resonance**

Neutrons are produced by the interaction of photons with the vacuum chamber walls and other components. The neutron production depends on a threshold energy which varies from 10 to 19 MeV for light nuclei, and from 4 to 6 MeV for heavy nuclei. Between threshold and approximately 30 MeV, neutrons are produced from a process known as *EI giant resonance*. This process will take place when the energy of the photon is transferred to the nucleus by inducing an oscillation in which the protons as a group move oppositely to the neutrons as a group. The energy of the peak is given by (Ref. 17);

$$E_o = 80A^{-1/3}$$

With the tube of the ALS made of ^{56}Fe , the peak energy of giant resonance is approximated at $E_o = 21$ MeV. The width of this peak varies from 3 MeV (heavy nuclei) to 10 MeV (light nuclei).

2.3.1 Skyshine Radiation

An important problem related to the giant resonance neutrons from the LBL Advance Light source is that of skyshine. The neutron dose from radiation generated by the source and transported by air-scattering to nearby general work area and the site boundaries and the effect of a shielding roof in reducing this "skyshine" is calculated. This work modeled the ALS source strength and source distribution, and employed the MORSE code to calculate the radiation transport and the skyshine doses (section 6.0). The first task was to make a real estimate of skyshine from a Ring source modeled after the ALS design. A first estimate, with no roof, was made to see the maximum amount of the skyshine radiation. Later several concrete roofs with different thicknesses were used to reduce the skyshine.

2.3.2 skyshine radiation for accelerators

In the design of accelerators which are enclosed in a separate building located at some distance from other buildings, a question often arises concerning the magnitude of shielding that is required for the roof over the shielding area. With an ordinary roof over the facility, there is a significant probability that radiation emitted upward and then reflected back from the atmosphere will exceed the dose-limit levels in the immediate area of the facility (Fig. 2.3). This reflected radiation is called *skyshine*. The radiation dose from gamma skyshine is estimated by the following equation (Ref.4):

$$D_{sd} = \frac{2.5 \times 10^{-2} \times D_{10} \times \Omega^{1.3}}{d_s^2} \quad (2.6)$$

where:

D_{sd} is the absorbed-dose index rate (rads $m^2 \text{ min}^{-1}$) from gamma skyshine.

Ω is the solid angle in Strds. subtended by the source.

D_{10} is the absorbed-dose index rate (rads $m^2 \text{ min}^{-1}$), measured in the upward direction from the X-ray source, at a standard reference distance of 1 meter.

d_s = distance from the source.

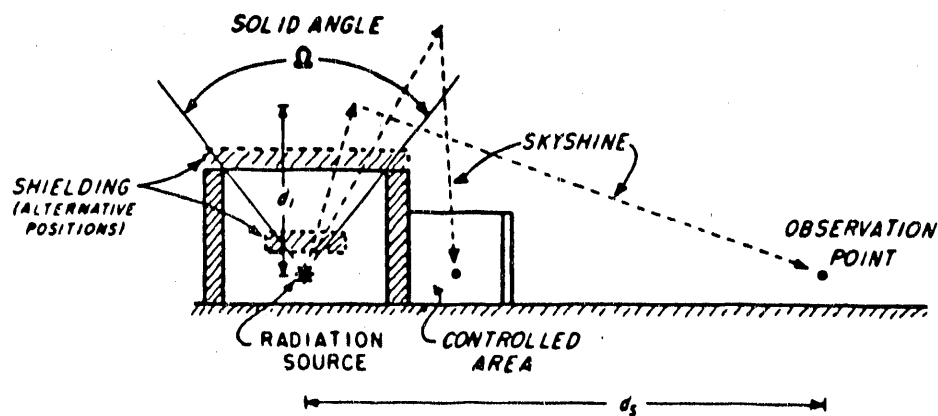


Figure 2.3. Schematic of skyshine from the Advance Light Source.

This relationship provides a conservative estimate for distances between 20 and 250 meters and for relatively low photon energies. It produces more accurate results for higher energy photons and shorter distances. Skyshine from neutron reaction can be estimated in a manner similar to the photon skyshine. The following equations have been used to do this (Ref 4):

$$\phi_{sd} = \frac{6.5 \times 10^{-2} \times \phi_0 \times \Omega}{2\pi d_s^{1.6}} \quad (2.7)$$

$$\phi_{sd} = \frac{5.4 \times 10^{-4} \times \phi_0 \times \Omega}{2\pi} \quad (2.8)$$

where d_s is the distance from the source to an observation point in meters.

ϕ_0 is the direct fluence.

Equation 2.7 is for distances greater than 20 meters and equation 2.8 is for the distances less than or equal to 20 meters. These equations relate to a point isotropic source of 5 MeV neutrons, but they provide a reasonable estimate of skyshine from neutrons of other energies. For purposes of calculating shielding the values obtained by equations 2.7 and 2.8, should be increased by a factor of two, to be conservative. By the use of the equation 2.7 and 2.8, the value of the skyshine was obtained as:

$$\phi_{sd} = 4.8 \times 10^{-8} n/cm^{-2} \cdot n$$

This value is later compared with the value obtained by the MORSE skyshine calculation.

2.4 High Energy Neutrons

Between about 140 MeV and up to a photon energy of about 1.1 GeV, The cross-section for photons on nuclei rises, allowing production of photopion. The largest peak happens at about 300 MeV with a width of about 110 MeV. This mechanism is due to the (γ, p) and (γ, n) reaction. The neutrons produced in these reactions tend to penetrate

much more than giant resonance neutrons, and at high energy accelerators these neutrons make more contribution to the direct dose outside of the concrete shield than neutrons from the giant resonance that make more contribution to the inside dose (Ref. 17).

3.0 ALS modeling for skyshine calculations

In order to implement the U.S. Department of Energy regulatory radiation limits in support of the ALARA, a long term limit of 100 mrem/year for all pathways has been considered. Levels of occupational exposure will be limited to 250 mrem/year, or 0.25 rem per 2000 hour worker year.

In calculation of the shielding, all the primary sources of radiation must be taken into the consideration. These sources are, *Giant Resonance Neutrons (GR)*, *High Energy Neutrons (HEN)*, and *photons*. The scope of this work, however, is limited to the resulting giant resonance neutrons and does not cover the HEN and photons.

3.1 Modeling the source and shielding geometry

Figure 3.1 models the Storage Ring source. The electron-ring is set at a radius of 30 m and 140 cm off the ground. Two concrete shielding walls, one on either side of the ring have been assumed. The architectural plan for the outer concrete wall is made to a 12-piece hexagonal shape. Each wall is 45 cm thick. The height of the walls are 244 cm (104 cm above the source). On the top of the walls, a proper roof thickness will be designed to cut the skyshine radiation to ALARA value. The complex system is arranged within the circular dome structure (building 6 of Lawrence Berkeley Lab) that contained the famous 184-inch cyclotron of E. O. Lawrence. The ALS dome structure is located close to other occupied buildings.

3.2 Modeling Source Strength for the Storage Ring

The LBL Light Source ring has to shield against both bremsstrahlung photons and neutrons. Both types of radiations result from the gradual beam loss during each storage cycle. The circulating beam was taken to be 3.3×10^{12} electron/fill, which gave a high energy source strength of 312 J/hr, assumed to be uniformly distributed along the

circumference of the Storage Ring. These numbers are based on the following assumptions:

- Maximum design Energy= 1.9 Gev.
- Conservative current=0.8 A.
- circumference = 197 m
- Filling cycle: two fills per 8-hr shift. giving a circulating electron beam of

$$\frac{0.8}{1.6 \times 10^{-19}} = 5 \times 10^{18} e^-/\text{sec}$$

$$n = \frac{3 \times 10^8}{197} = 1.52 \times 10^6 \text{ rev/sec}$$

$$N = \frac{5 \times 10^{18}}{1.52 \times 10^6} = 3.3 \times 10^{12} e^-/\text{fill}$$

so the total energy loss is:

$$E = 1.9 \text{ GeV} \times 1.6 \times 10^{-10} \times 3.3 \times 10^{12} = 1000 \text{ J/fill}$$

$$\frac{2}{8} \text{ fill/hr} \times 1000 \text{ J/fill} = 250 \text{ J/hr}$$

$$250 \text{ J/hr} \times 1.25 = 312 \text{ J/hr}$$

The values were then increased by a factor of 1.25 to account for additional loss of beam at injector.

The neutron source strength is obtained from the beam-loss power by a constant conversion factor derived by Swanson ref. 7;

- From reference 7, the neutron yield is

$$Y = 1.21 \times 10^{11} Z^{0.66} n/(\text{sec.KW}) \quad (3.1)$$

where Z is the atomic number of the material lining the electron vacuum tube. Swanson estimates an overall error in neutron yield less than 20% for all materials. For Fe, the principal component of the vacuum chamber,

$$Y = 1.21 \times 10^{11} \times 26^{0.66} = 1.0 \times 10^{12} \text{ n/s-kw},$$

or 1×10^9 photoneutrons per Joule of electron beam lost uniformly around the Storage-Ring circumference. The total neutron yield from the beam dump into the vacuum chamber (Fe) is:

$$Q = 1.0 \times 10^9 \text{ n/J} \times 312 \text{ J/hr} = 3.12 \times 10^{11} \text{ n/hr}$$

$$Q = 3.12 \times 10^{11} \text{ n/hr} \times \frac{1}{3600} = 8.7 \times 10^7 \text{ n/sec}$$

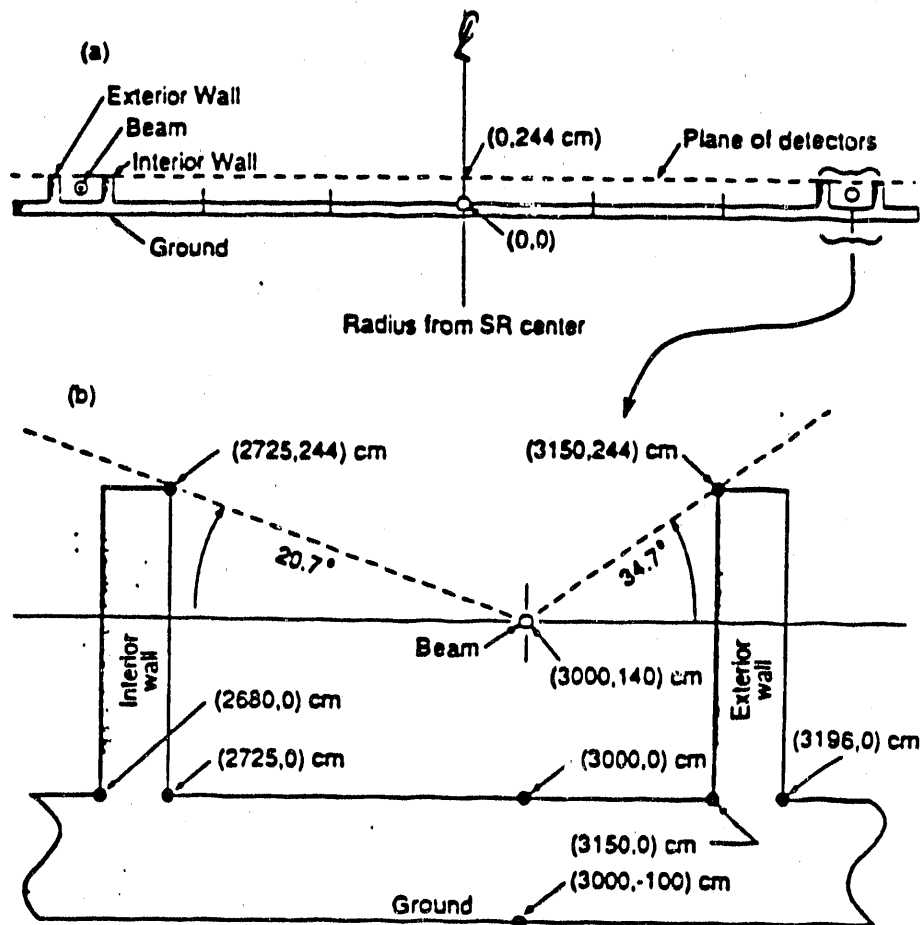


Figure 3.1. Neutron source is the circular Storage Ring at 30 m radius. Cross section shows the ring in relation to ground and two 45-cm thick circular walls. A roof that is analyzed in the calculations, is not shown in this figure.

These neutrons have a nuclear boil-off spectrum similar to the spectrum of neutrons emitted by a highly excited fission fragment, and are assumed to have the spectrum shape of ^{252}Cf fission neutrons. The giant resonance neutrons are assumed to have an energy range of thermal to 19 MeV, with a energy peak of 2-3 MeV, and average energy of 1.5 MeV (Ref. 20).

4.0 MORSE MONTE-CARLO

4.1 Description of MORSE CODE

The MORSE code is a Monte-Carlo program for neutron transport. The version which has been used to calculate the ALS skyshine, MORSE-CG, is described in the Radiation Shielding Information Center (RSIC) manual CCC-203C&D (RSIC84). It is written in FORTRAN IV (appendix A1.0). As described in RSIC84, MORSE is a multipurpose neutron and gamma ray transport Monte Carlo code which is designed to solve a variety of complicated shielding problems. Through the use of multigroup cross-sections, the solution of neutron, gamma ray, or coupled neutron neutron-gamma ray problems may be obtained in either the forward or adjoint mode. Morse has the capability of using a three-dimensional geometry with an albedo option available at any material surface. Isotropic or anisotropic scattering up to P_{16} expansion of angular distribution is allowed. Also MORSE contains a combinatorial-geometry software package to simulate a wide range of geometric configurations. A variety of neutron estimators can be implemented. For example:

1. Boundary-crossing estimators,
2. Point detector, "next event" estimators
3. Track-length estimators.

Each or any of these estimators can be weighted by arbitrary spectrum-weighted factors that convert neutron numbers to fluence and dose-equivalent.

4.1.1 Boundary Crossing Estimator

Boundary-crossing is the simplest neutron estimator used by MORSE. It defines the flux by a summation over all neutrons crossing a given surface region of a random AREA:

$$\phi = \frac{\sum \text{WATE} / \cos(\theta)}{\text{AREA}} \quad (4.1)$$

where ϕ is the neutron fluence, WATE is the weight of each individual neutron that crosses the AREA and θ is the angle between the neutron direction and the perpendicular to the surface which the neutron is crossing.

4.1.2 Point-detector Estimators

When it is desired to use Monte-Carlo techniques to estimate particle fluence at a point in space. The method described in MORSE is called the "next event" estimator. It scores from each collision point the analytical probability of the next arrival at the detector. The theoretical basis of the technique is reviewed briefly as follows. A particle state is described in "phase space" by location, X, Y, Z, a set of direction cosines U, V, W, and energy group IG. The random walk process in Monte-Carlo generates a sequence of interactions and collisions that are samples from an event density function, $P(\Omega)$, where Ω is the solid angle description. This probability function contains particle birth and the condition of an event at a point, described as the new "phase space" coordinates. For this event the fluence ϕ at the "detector", is defined as:

$$\phi = P(\Omega) \times \frac{\exp - \sum \lambda_i r_i}{\sum r_i^2} \quad (4.2)$$

where r_i is the particle distance from a point in the phase space to the detector and λ_i is the interaction probability of the particle from the phase space to the point detector coordinates. This is computed even if there are several media, i, for the vector needed to

connect the particle description and the detector location.

Point detector estimators at MORSE-CG are described in two subroutines, RELCOL and SDATA, using the next event estimator to score from source and collision events respectively. In RELCOL, the fluence estimate from a normal particle collision is given by

$$\Phi = \frac{WATE e^{ARG} P(COSSCT,IGO)}{r^2} \quad (4.3)$$

where

- Φ is the fluence from one collision.
- WATE is the statistical weight of the particle of the collision.
- ARG is the negative no. of mean free paths from collision to detector.
- $P(COSSCT,IGO)$ is the probability, per steradian, for a particle in the incoming group IGO scattering to a lower energy group through the angle $\cos^{-1}(COSSCT)$. The subroutine RELCOL is called by user at real collision, through subroutine BANKR with the value of NBNKID=5.

The subroutine SDATA estimates the fluence at point detectors made for each original particle event. This is an isotropic source with X, Y, Z location. Fluence is given by:

$$\phi = \frac{WATE e^{ARG}}{4\pi r^2} \quad (4.4)$$

This subroutine is also called by BANKR with the value of the NBNKID=1. For the ALS source distribution, an isotropic uniform ring source is considered in the subroutine SOURCE.

4.3 Cross_Section sets

In the very first run of MORSE at Lawrence Berkeley Lab, the 22-group cross-section set for neutrons for air was taken from one of the sample problems provided with the first version of MORSE. The main purpose of this run was to test that the implementation of MORSE was on the correct course, in particular it confirmed that the input data file, and especially the initial geometry arrangement were set up correctly for the ALS skyshine problem. The materials list available for the first run included 22-group neutron cross-section only for air, vacuum, and impervium. *Impervium* is a fictitious material with the computational property that neutrons incident on it are not transported or considered further. *Vacuum* is a material that allows neutrons to continue within its volume without any change in energy or direction.

Subsequent, production, runs were made using 37-group neutron cross-sections for a large variety of elements and mixture-based cross_sections. According to RSIC, the neutron groups are made to allow for the major peaks and valleys in total neutron cross-section of nitrogen, oxygen, silicon and iron. A set of response functions useful in radiation transport applications is also included as part of the library from RSIC77(Ref.5). The library is based on cross_section data from the DNA working cross_section library and the Evaluated Nuclear Data File(Ref.5). The 37 neutron groups range from 4.14×10^{-1} eV (thermal) to 19.64 MeV. The set of cross-section contains a total of 41 nuclides and angular distribution in the form of Legendre coefficients to order P_3 .

Mixtures of elemental materials, are made directly in the MORSE code in the data file in each run. The composition of concrete was taken from Report NCRP-38 (NCRP71) using the overall density $\rho=2.26 \text{ g/cm}^{-3}$. The atom densities of the different materials are inputed in the units of atom/barn-cm. since the unit of cross-sections are in barns, the interaction probability per unit particle path distance will be in reciprocal centimeters. For air, the percentage for N_2 and O_2 are assumed to be 78.06% and 20.99% by

Table 2. Compositions of concrete and air as used.(*)

Concrete	Air		
Si	2.015×10^{-2}	N	4.195×10^{-5}
O	4.587×10^{-2}	O	1.128×10^{-5}
Al	1.743×10^{-3}	—	—
H	1.375×10^{-2}	—	—
Ca	2.660×10^{-3}	—	—

(*) Nuclei per cm^3 , multiplies by 1×10^{-24} .

volume. A sample calculation of atom densities is included, for example for air:

$$\frac{6.023 \times 10^{23}}{2.2414 \times 10^4} \times (0.7806) \times 2N\text{mol}^{-1} = 4.195 \times 10^{19} \text{ Ncm}^{-3}$$

where:

- 6.023×10^{23} is Avogadro's number
- $2.2414 \times 10^4 \text{ cm}^{-3}$ is the ideal gas at STP.

The same terminology was used for oxygen to derive the atom density.

4.4 Conversion of spectra to Dose Equivalents

In Figure 4.1, dose equivalents are calculated from the spectra generated for the condition of figure 4.2 in two ways. The points "C" obtained using a single fixed conversion factor proposed for ^{252}Cf (ICRP73,table 9). Comparing these values with points "2" of figure 4.2 it can be seen that they are identical. Points "I" of figure 4.1 are obtained by folding neutron spectra at each detector with energy dependent conversion factor of ICRP73.

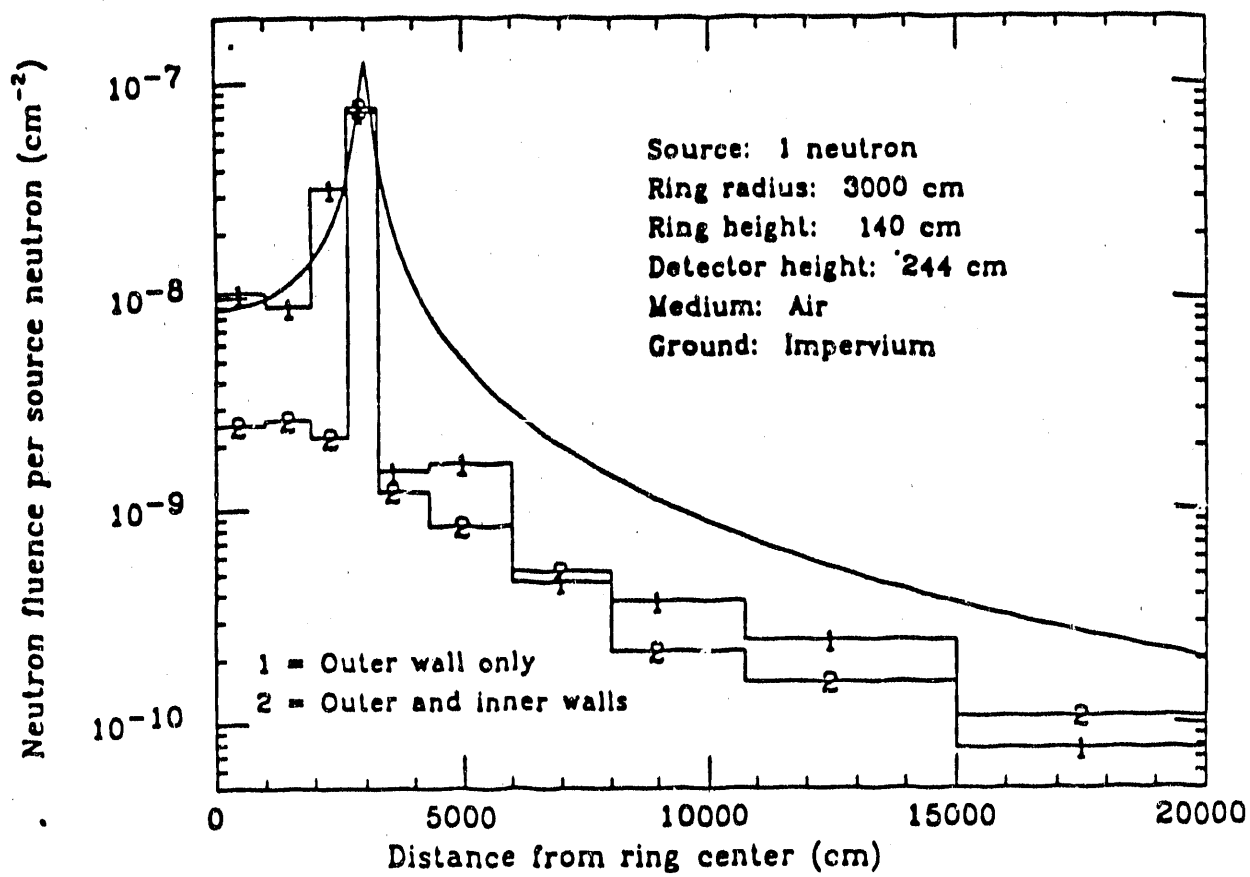


Figure 4.1, skyshine dose-equivalent for two impervium walls. Two different fluence to dose conversion factors are compared "C" is the constant factor, "I" is the energy variable factor from ICRP-21 folded together with neutron spectra.

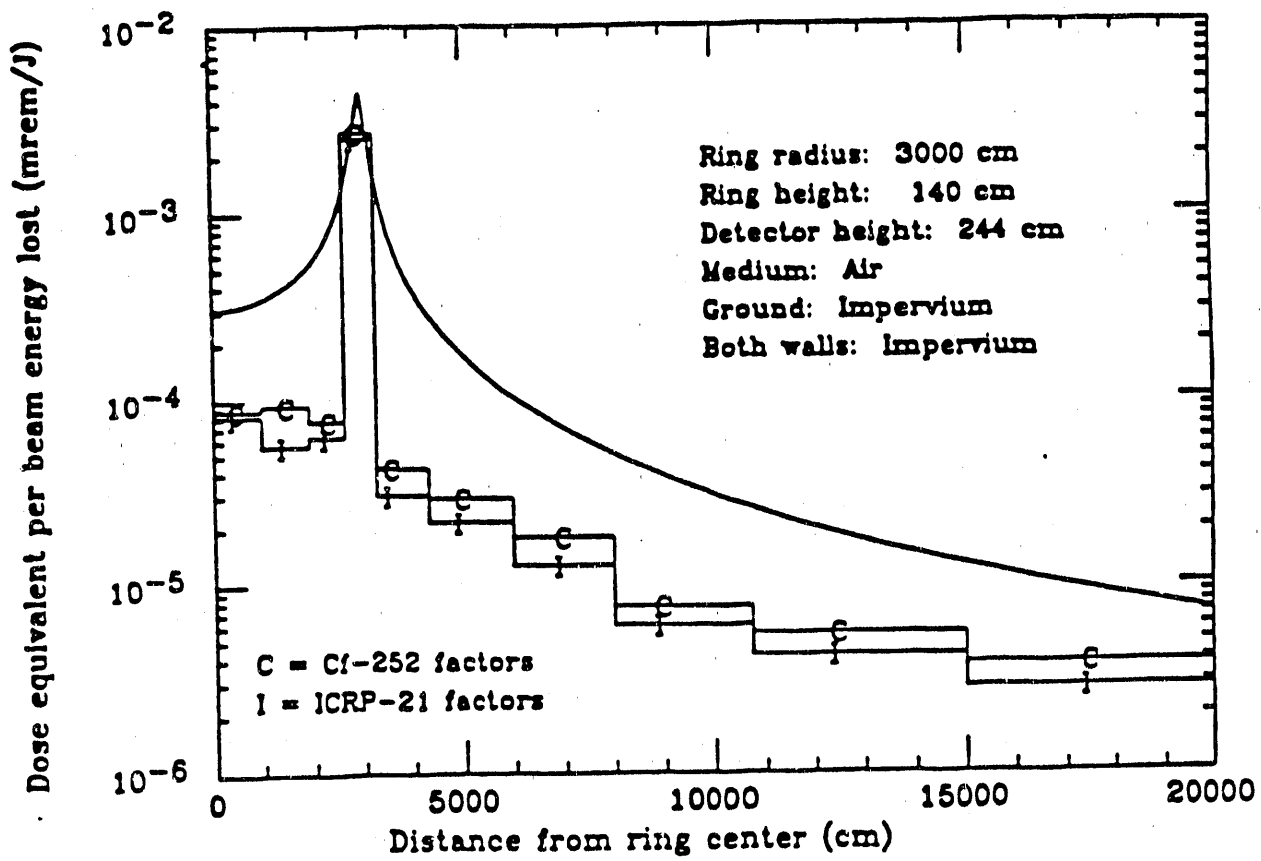


Figure 4.2, Neutron fluence due to skyshine with impervium ground and shielding walls. Air fills all other spaces. 1) Only exterior shield wall is set to impervium. 2) Interior and exterior walls are impervium.

The detector at 3000 cm, directly above the beam, is the only detector to see the direct source, which gave almost identical dose-equivalent values (within about 10%). For every other detectors, which receive only air scattered spectra, the spectral-folded dose-equivalents, "I"*, are about 25 - 30% below the dose-equivalents, "C", which are obtained using a constant factor.

- The conversion assumed from ICRP73 for a ^{252}Cf neutron spectrum is, $19 \text{ n/cm}^{-2}\text{sec}^{-1} = 2 \text{ mrem/hr.}$

These factors yield an overall conversion factor used for these calculations:

$$H(\text{mrem}) = 3.51 \times 10^4 \times \phi(\text{cm}^{-2}) \times U(\text{J}) \quad (14)$$

Where U is the total electron beam energy loss in Joules.

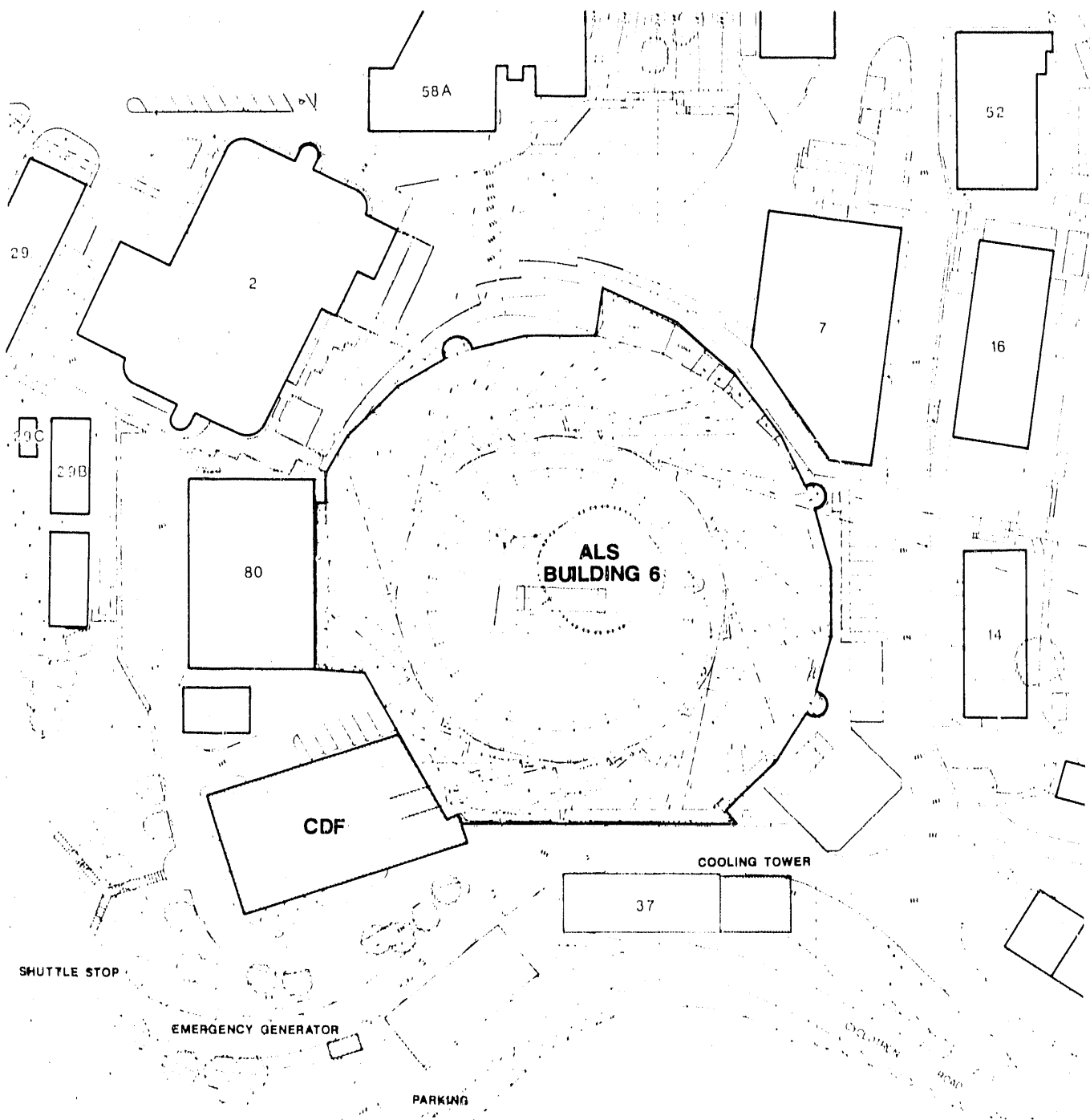
4.5 MORSE Shielding Geometry

A general description of the Lawrence Berkeley Laboratory Advance Light Source design is shown in figure 4.3. The complex system is arranged within the circular dome structure. The dome structure is surrounded by other adjacent buildings. The systems that contribute most to radiation problems are:

- linac, that brings low energy electron up to 50 MeV to transport to the Booster Ring.
- The Booster Ring, that accelerates electron beam from 50 MeV to 1500 MeV before transferring them into the Storage Ring.
- Storage Ring, that stores electron beams at energies in the range 1500-1900 MeV.

As this work is focused on the skyshine from the Storage Ring. It does not include the LINAC and the Booster Ring. They are only mentioned as other possible sources of radiation.

*Appendix A1.2.3



XBL 901-313

Figure 4.3 plan view of ALS facilities, as set in existing circular dome building at LBL and surrounded by other buildings. Important radiation sources are :
Electron Linac, Booster ring, and Storage Ring.

Although the outside concrete shielding designed for the Storage Ring was a "ratchet" design with various distances from the beam to nearest wall, an average circular geometry was chosen for calculational simplicity. Because of general spreading loss of electron beams assumed for circular rings, simple calculation of skyshine fluence and dose-equivalent are very difficult to treat. This is the reason that MORSE code was employed. Figure 3.1 shows the shielding geometry used for the Storage Ring of the ALS facility. The electron ring is set at a radius of 3000 cm (30 m) and 140 cm off the ground. A ring shield wall is set up around the ring on the both sides. Two shielding walls, one on either side of the ring have been assumed. The walls are 45-cm thick (they are set between the radii of 2680 and 2725 cm for the first wall and 3150 and 3195 cm for the second wall in the MORSE input file). The entire arrangement is then enclosed in a calculation boundary, an enveloping spherical shell (set between the radii of the 25000 and 30,000 cm). The enveloping shell is considered to be vacuum to cause neutrons reaching that radius to be totally absorbed and vanished. The ground floor is concrete, 100 cm thick. The effect of each component ground, interior wall and exterior wall could be tested by assuming to be made of vacuum in the MORSE calculation.

4.6 MORSE detector geometry for Storage Ring

There were two arrangements of detector geometry for the Storage Ring skyshine calculations. In each arrangement a total of 11 and 12 detector were used respectively. (A third set of detectors was used for shielding calculation, which will be explained in section 7.).

To input the detector geometry parameter into the MORSE geometry, three values are necessary X, Y, Z (Fig. 4.4). X, is the horizontal distance from the center of the ring to the detector. Y, is the orthognol horizontal coordinate. Z, is the height of the detector above the ground. The value of the Y in the two detector arrangements was zero, because the detectors are placed on the X-axis.

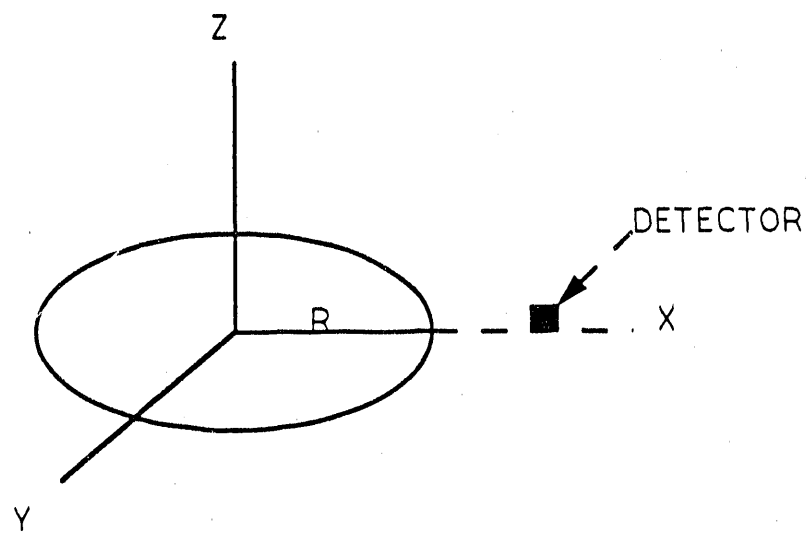


Figure 4.4, X, Y, Z direction of a detector relative to a ring source.

1. In the first detector geometry Z was set at 244 cm, and X was set as a function of radial distance from the ring source up to 200 m measured from the ring center as follows: (figure 4.5)

- The detectors, 1-3 were set inside the ring at radii $X=0.0, 500, 1500$ cm respectively.
- Detector 4 was set directly above the beam at $X=3000$ cm. (When a roof was added the value of Z; for this detector only, was increased by the roof thickness)
- Detectors 5-11, were set outside of the ring at radii $X=3600, 5000, 7000, 9000, 12500, 17500, 20000$ cm.

Detectors 1-5 were located within the source, and detectors 6-11 were located within the site boundary.

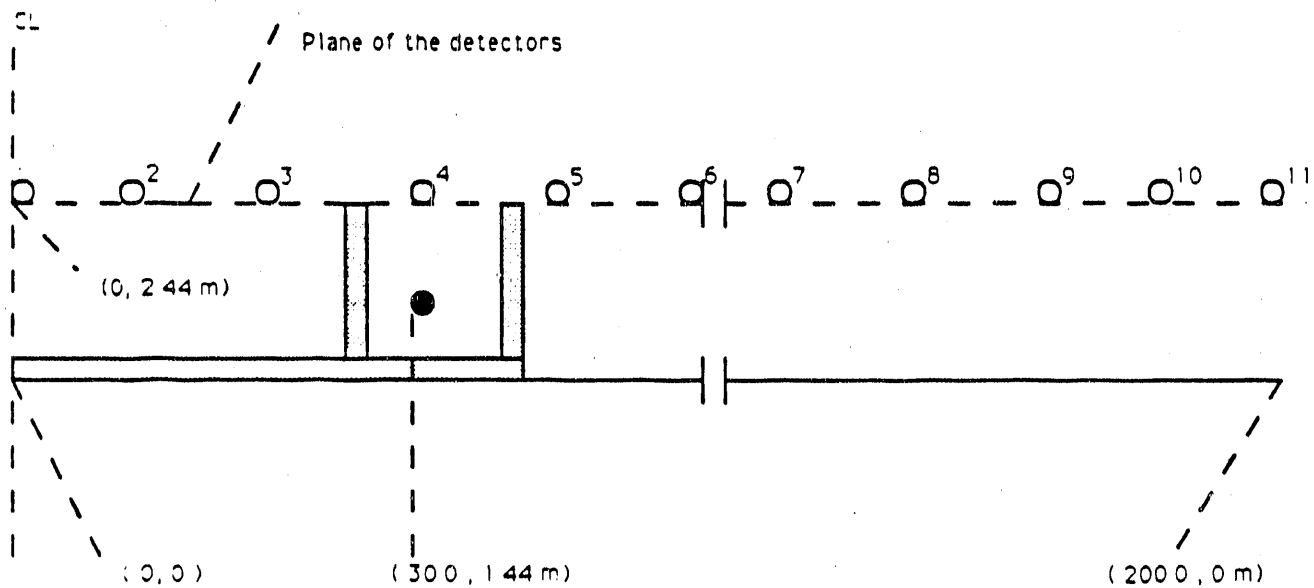


FIGURE 4.5, Radial detector geometry, from the ring center to a distance of 200 m (total of 11 detectors).

2. The second detector arrangement was set as the function of altitude (figure 4.6).

The objective of this detector location was to see the effect of skyshine radiation at site boundaries and nearby occupied areas. There were a total of 12 detector locations, were used at 39 and 50 m measured radially from the ring center as follows:

- detectors 1-6, were set at 39 m from the ring center, $X = 3,900$ cm, $Y = 0.0$, with the following heights respectively: $Z= 0.0, 244.0, 500.0, 1000.0, 1500.0, 2000.0$ cm.
- detectors 7-12, were set at 50 m from the ring center, $X = 5,000$, $Y = 0.0$, with the following heights respectively: $Z=0.0, 244.0, 500.0, 1000.0, 1500.0, 2000.0$ cm.

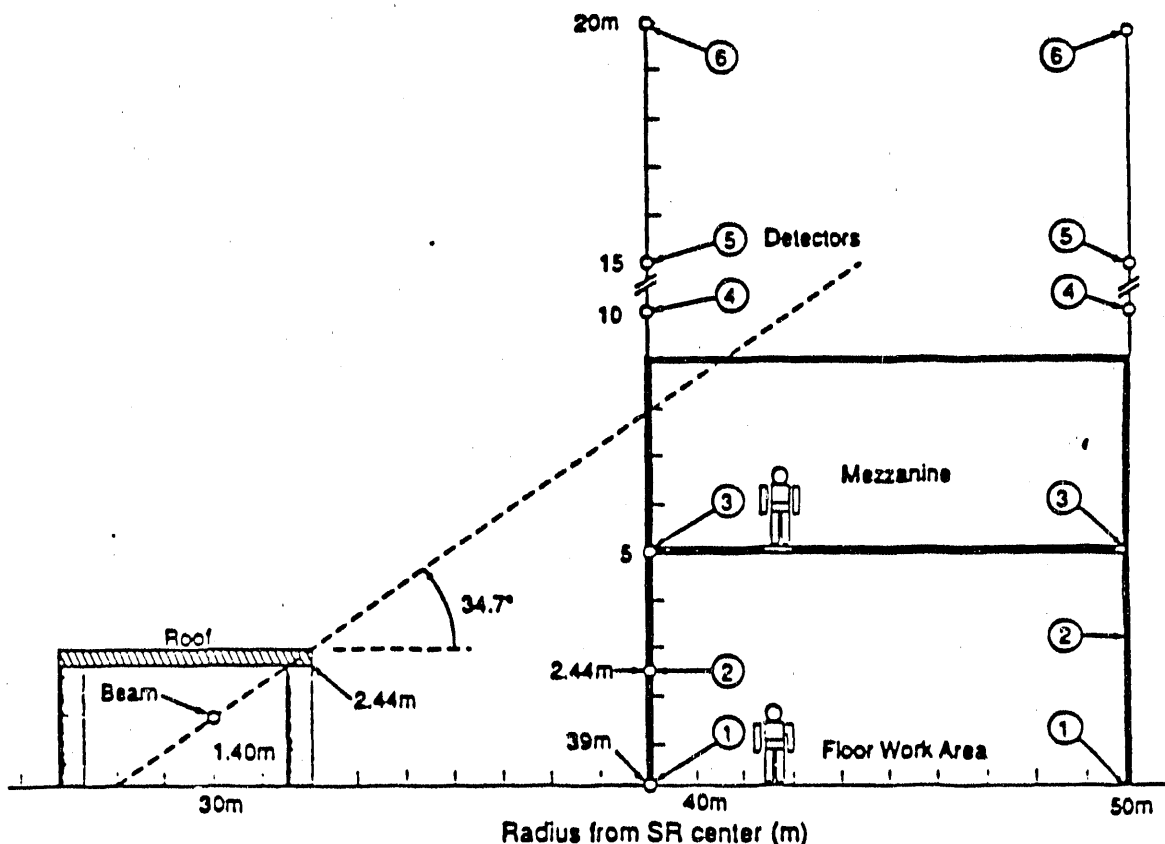


Figure 4.6. Vertical detector geometry. Beam is at 30 m radius, with the height of 1.4 m. Occupied areas (two floors) are between 39 m to 50 m. 34.7° is the angle of a ray that just misses the outside shielding walls.

5.0 IMPLEMENTATION OF MORSE

5.1 Commissioning Tests with Vacuum and Air

Figure 5.1 shows the first result from a MORSE run. In this run the detectors were set at the height of 244 cm, which give the skyshine fluence at this height. This run is done for no materials in the ring vicinity, and only vacuum through the enveloping spherical shell. The MORSE Monte-Carlo fluence results can therefore be compared with the following geometrical formula:

$$\phi = \frac{N}{4\pi\bar{d}^2} \quad (5.1)$$

where N is the number of particles produced by a uniform ring source and \bar{d}^{-2} is the average inverse distance squared. It comes from the following relation:

$$\bar{d}^{-2} = [(R^2 - R_0^2)^2 + 2\Delta Z^2(R^2 + R_0^2) + \Delta Z^4]^{-1/2} \quad (5.2)$$

where:

- R_0 is ring radius = "3000" cm
- ΔZ is the vertical distance from the ring to the detector = (244-140) = 104 cm.
- R is the variable radius of the detector, measured from ring center.

For the analytical as well as Monte-Carlo calculations a uniform beam loss is assumed around the Storage Ring circumference. The result of the above calculation is shown as a solid curve in Figure 5.1. The peak of the curve is at 3000 cm the radius of the ring source. The Monte-Carlo distribution specified by "V" agrees closely with the solid curve. This was also a test for the geometry, source implementation and boundary crossing programmed within MORSE (by subroutine BANKR in appendix A1.1.4).

This run was made for air as well as vacuum. The comparison of results with *air* and *vacuum* are close except at larger distances.

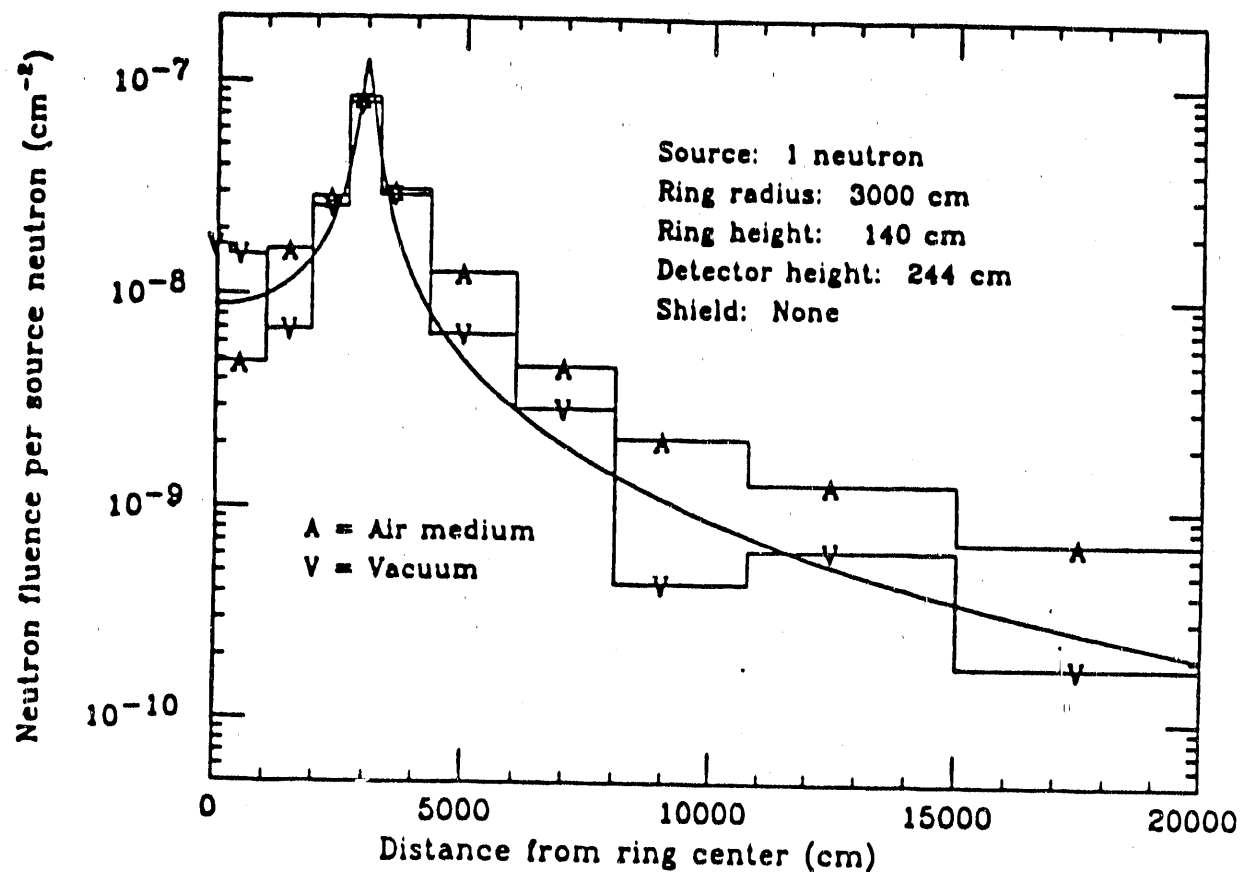


Figure 5.1. Neutron fluence at 244 cm height above ground as a function of distance from ring center. No shielding material is used for these calculations, except air.

Near the source results are close, because the attenuation of air is not significant. As distance gets greater the air scattering of the neutron becomes significant. An increase of 2 to 5 is seen in the range of $R = 5000$ to $20,000$ cm from the ring center. Figure 5.2 is the same data with values of the fluence converted to dose equivalent.

The results of the calculations using *impervium* (impenetrable shielding) are shown by figure 5.3. Using ground and shielding walls from *impervium* makes the following changes:

- Single exterior wall reduces the fluence by about a factor of 10 beyond 5000 cm (point 1 to A).
- The reduction in fluence is greater by a factor of 20 closer to the exterior wall (point 1 to A).
- with impervium, within the ring interior there is no effect.
- If another impervium wall is added, the reduction outside of the wall is not affected.

5.2 first results with Air and Concrete

After all the commissioning test were made with vacuum and *impervium*, the realistic construction data (with air and concrete) was put into the data file. There were significant differences observed in comparison to the previous tests. Different sized batches of neutrons were chosen for the testing (ranging from 2000 to 10,000 neutrons). The final results were run with 10,000 neutrons, giving a proportionate increase in the CPU time. Concrete absorbs about half of the neutrons hitting it. This creates a significant large-area albedo effect (the other half scatter from the surface). The albedo neutrons are characterized by a $1/E$ slowing-down distribution and mix with a big portion of the direct-source spectrum. At larger distances away from the shield fluence increased by a factor of 3-6. The largest observed increase was at about the 200 m radius from the ring center (fig. 5.4).

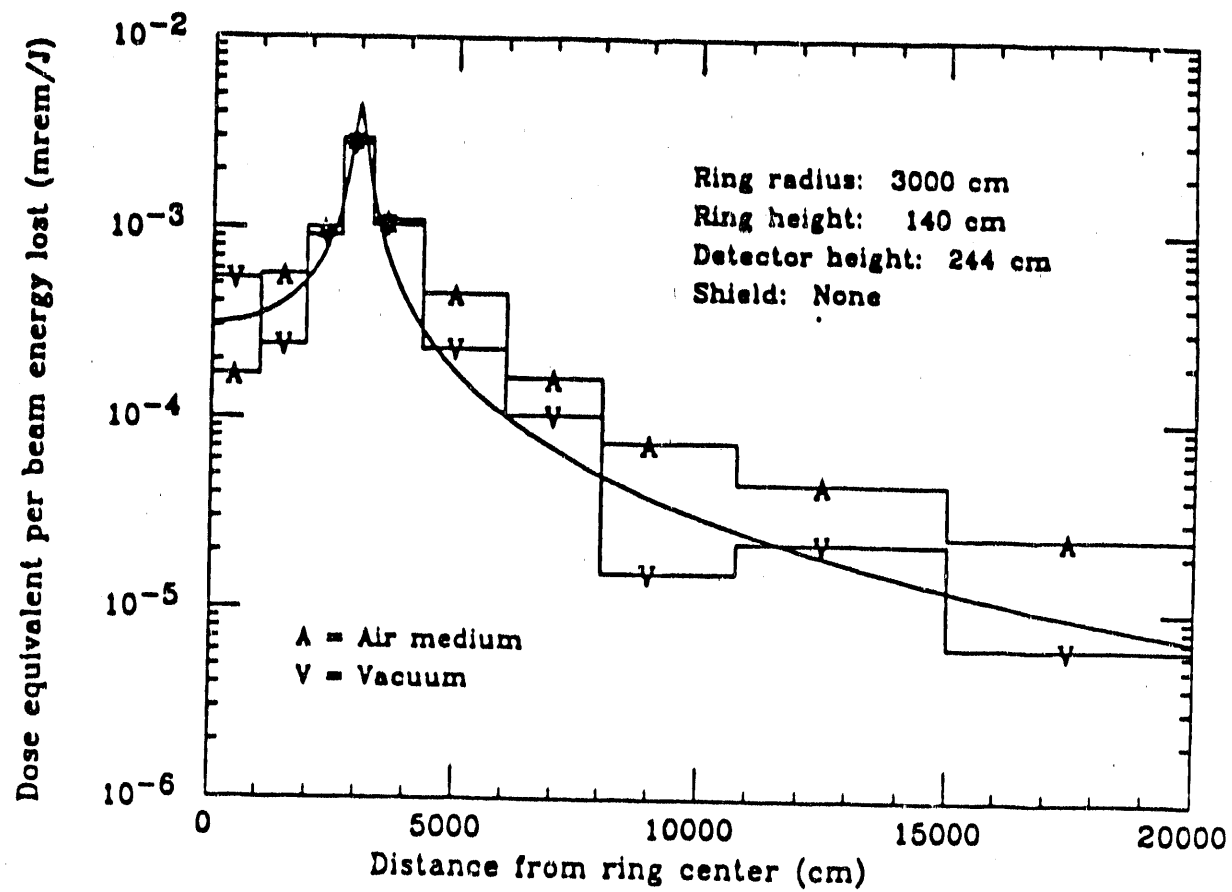


Figure 5.2. Dose-equivalent for two diffuse materials, air and vacuum.

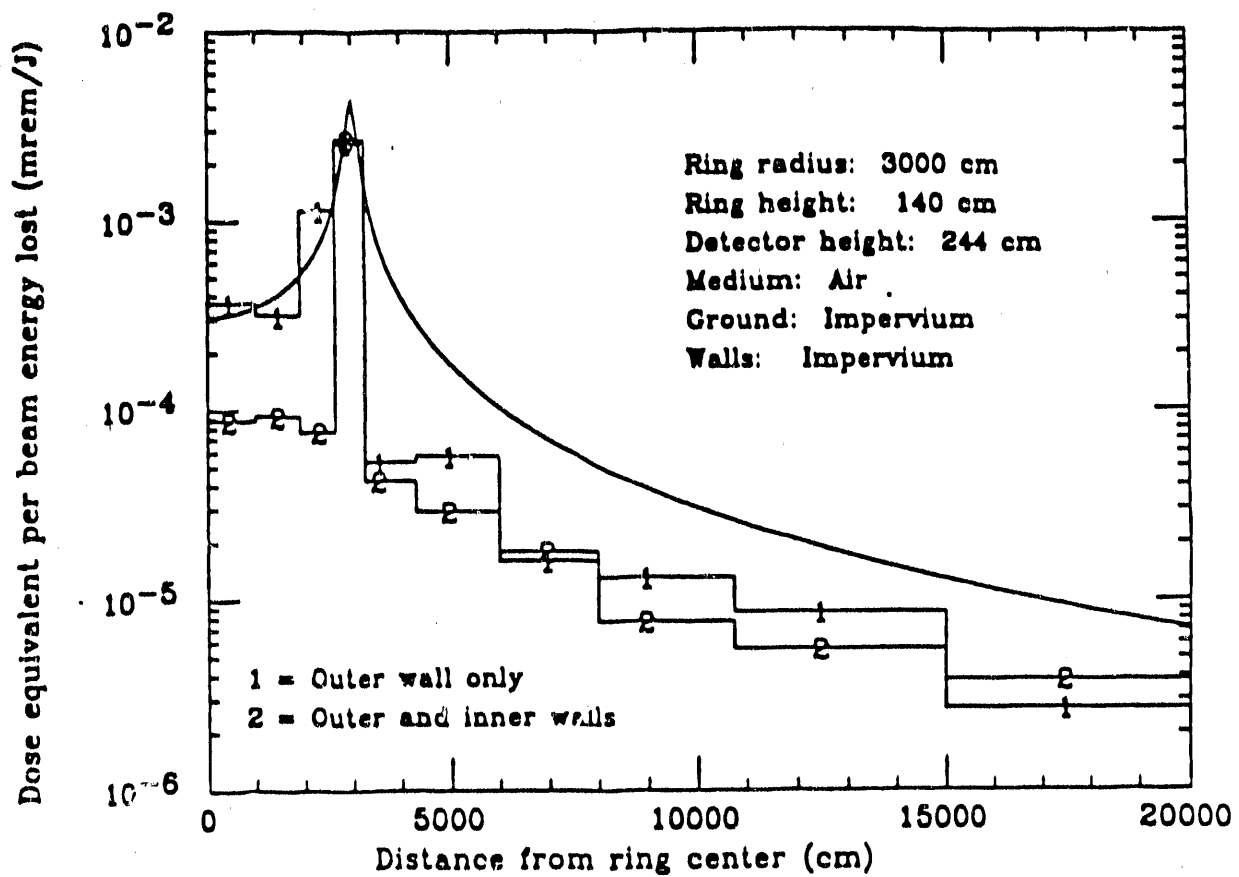


Figure 5.3. Dose-equivalent as a function of distance from ring center using imperium walls and ground.

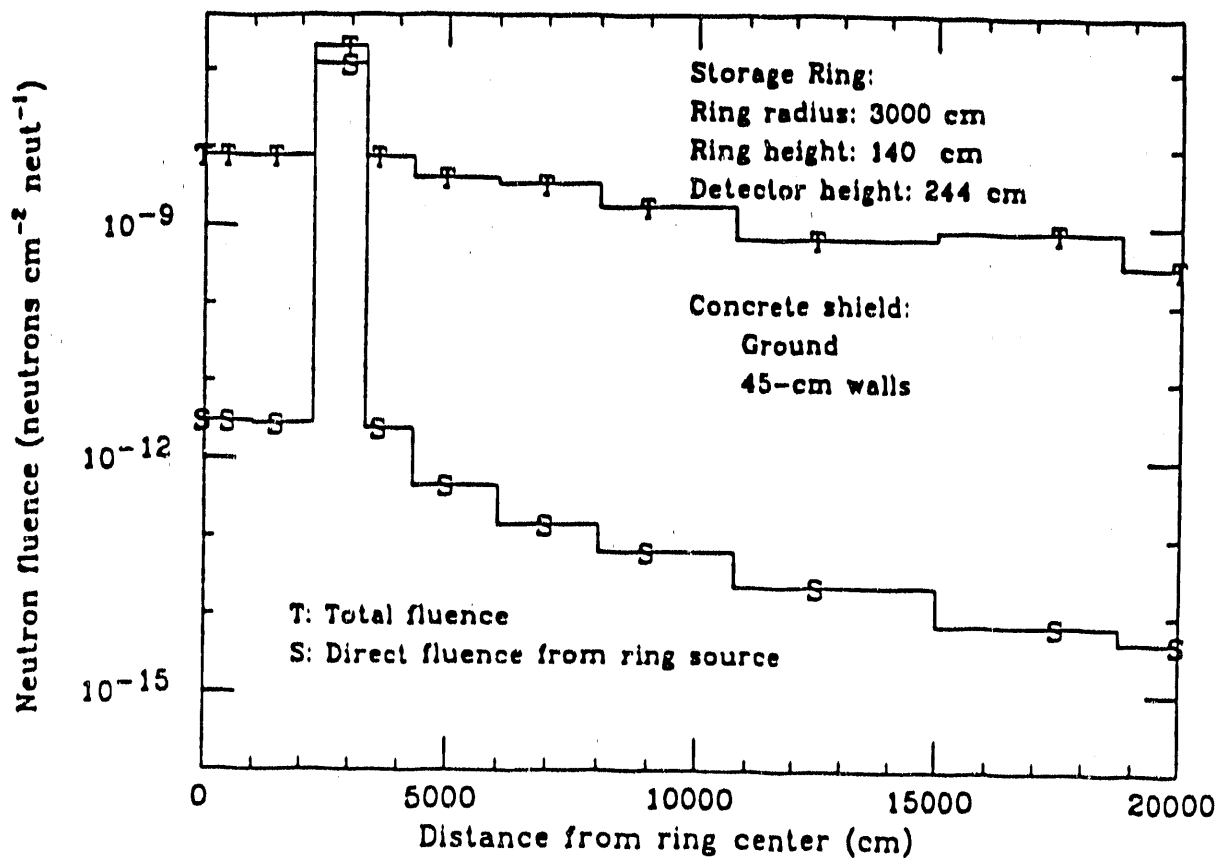


Figure 5.4. Neutron fluence as a function of distance from ring center for no roof, and concrete walls and ground. Data are normalized to one uniform photoneutron from Storage Ring.

6.0 RESULTS OF SKYSHINE CALCULATIONS FROM STORAGE RING

The calculations of neutron skyshine fluence were first normalized to a single photon-neutron, uniformly distributed around the ring circumferences. The results are expressed in terms of both neutron fluence and dose equivalent for two cases: 1) with no roof and 2) a 30-cm thick roof placed on the top the Storage Ring at a height of 244 cm. A 15-cm roof was also used for a primitive comparison of skyshine radiation.

6.1 neutron fluence and dose-equivalent no roof (radial distance)

Figure 5.4 shows the neutron fluence as a function of radial distance. Inside the ring there is very little variation of fluence with radius. A big jump in the fluence is observed right above the beam. The fluence observed at 30 m from the ring source (detector directly above the ring source) exceeds the nearby fluences by 5 decades (fig. 5.4). The data indicated by T are the total fluence (direct plus the scattered neutron fluence). Data indicated by S are the direct fluence (neutron contributions direct from the source). Due to the absence of the roof, There is only a small variation between S and T.

The differences between S and T for distances greater than 40 m from the ring center are much larger. The difference between the fluences is from the effect of the exterior wall. The same difference is also obvious within the ring source (0 to 24 m). Figure 6.1 shows the dose equivalent as a function of radial distance, the dose equivalent is obtained by using a single conversion factor of fluence to dose (section 4.4). It follows the same exact variation as fluence.

6.2 neutron fluence and dose-equivalent no roof (as function of altitude)

Figure 4.5 illustrates the location of the Mezzanine in relation to the ring source and the shielding walls. The arrangement of the detectors is different in this run. As explained before, the detector arrays were set at 39 and 50 meter (approximate distance of Mezzanine walls from the Storage Beam center). Detector heights were set at vertical distance of 0, 2.44, 5, 10, 15, and 20 meters.

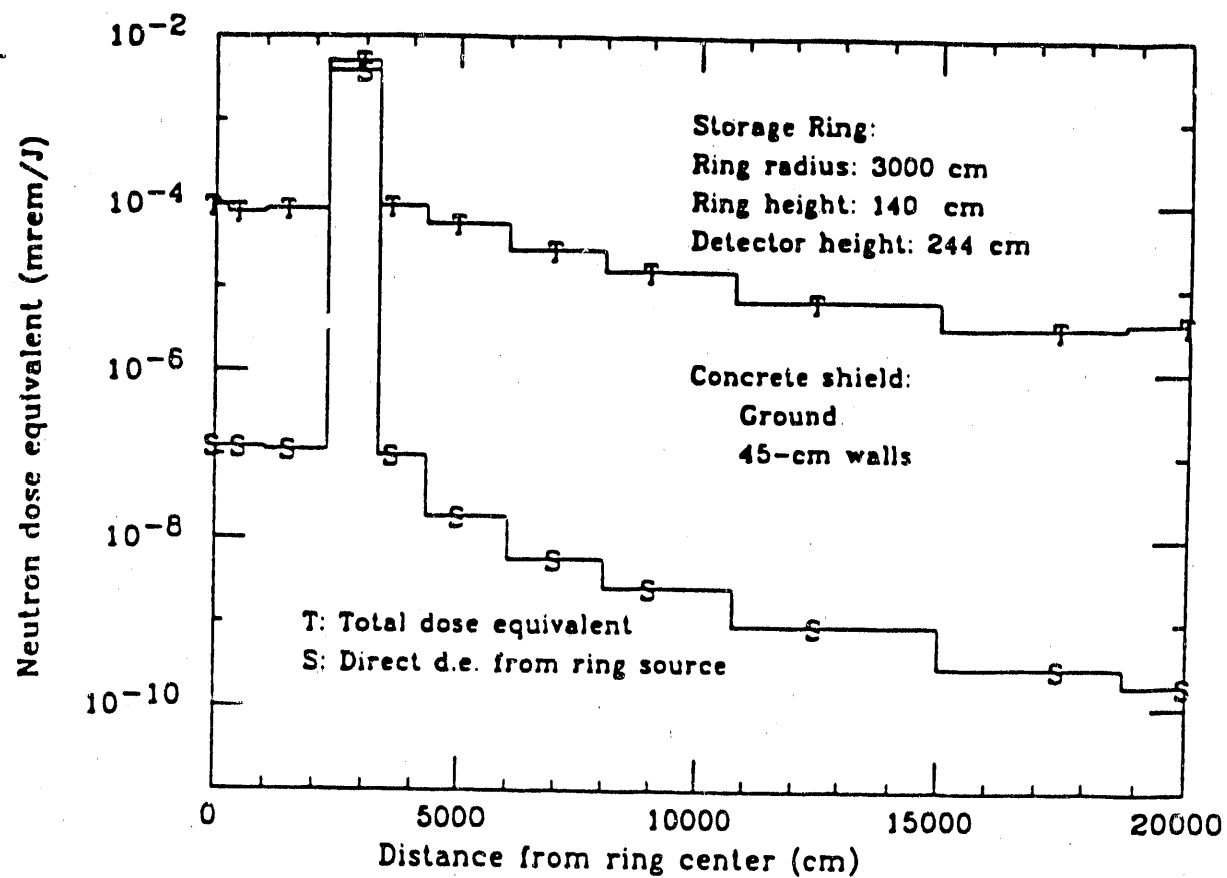


Figure 6.1, Neutron dose-equivalent as a function of distance from ring center (no roof).

At 39 m from the ring center, the neutron direct radiation that just misses the wall is at about 8 m above the ground (Fig. 4.5), so direct fluence contributes significantly for heights above the 8 m.

The variation of fluence and dose equivalent as functions of height above ground level are shown in figures 6.2-6.5. As can be seen from figure 6.2 (R=39) the direct fluence S is negligibly small compared to the total fluence, T at ground level. The magnitude of the total fluence reaches its highest value in the height range of 9 m to 13 m, which is the location of Mezzanine (occupied areas). The difference between the total fluence T , and the direct contribution S indicates the skyshine fluence. At ground level almost all the contribution is from the skyshine but with the increase of altitude (4 to 20 m), the direct fluence contribution will increase (because there is no roof the direct fluence quickly rises as a function of height). from the figure 6.2 , it can be seen that, the skyshine fluence averages about 73% of the total fluence and the rest is the direct fluence.

At low height, between 0 and 2.44 m, the direct fluence must penetrate the concrete shield wall ; (The direct distribution includes only neutrons that don't scatter, either in the air or either the concrete walls).

The results of the 39 and 50 m detector locations are comparable. Figure 6.3 shows the total and direct fluence at 50 m detector location. This location like the 39 m location, shows negligible direct fluence at ground level, but the skyshine fluence averages about 83% of the total fluence from 4-20 m off the ground. The skyshine fluence shows a 50% reduction comparing to the skyshine at 39 m location. Figures 6.4 and 6.5 are the resulting dose equivalent obtained by the fluence.

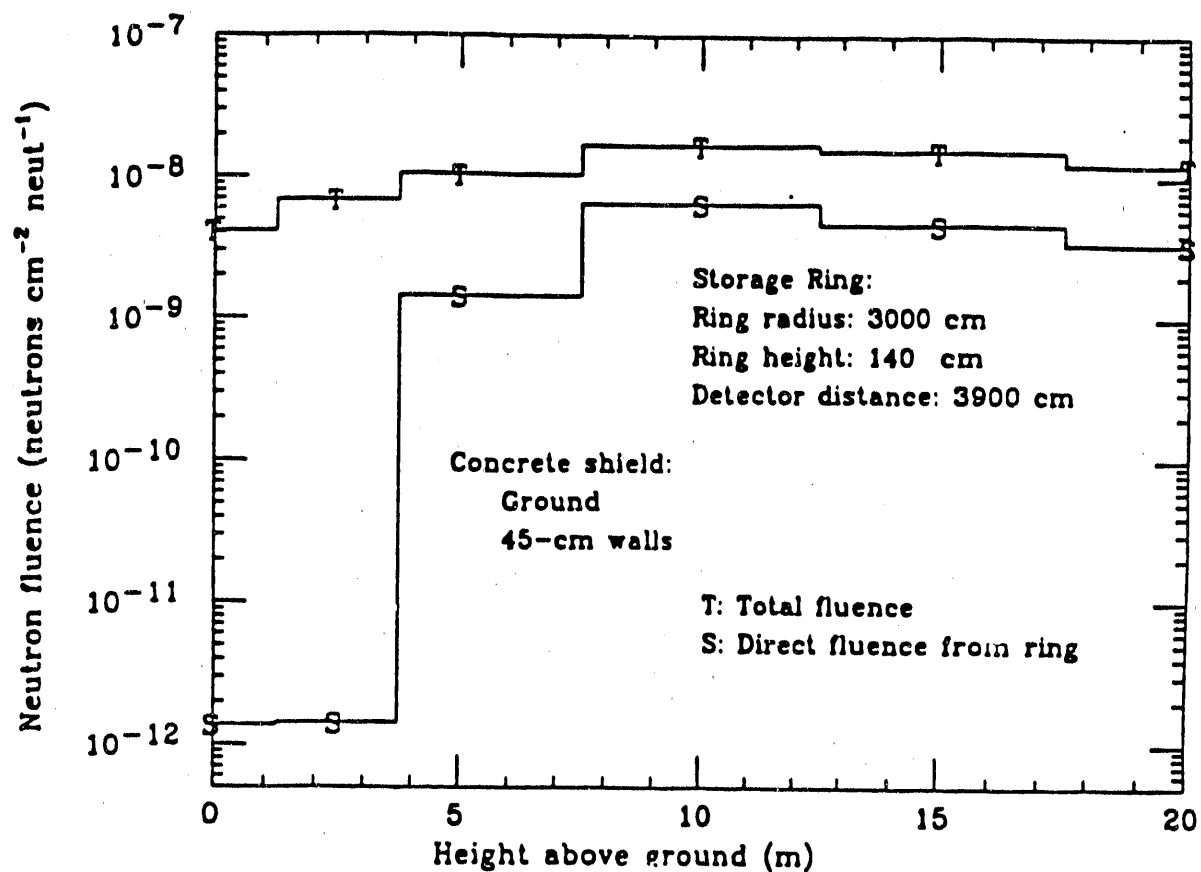


Figure 6.2. Neutron fluence as a function of height. Radius set at 39-m no roof.

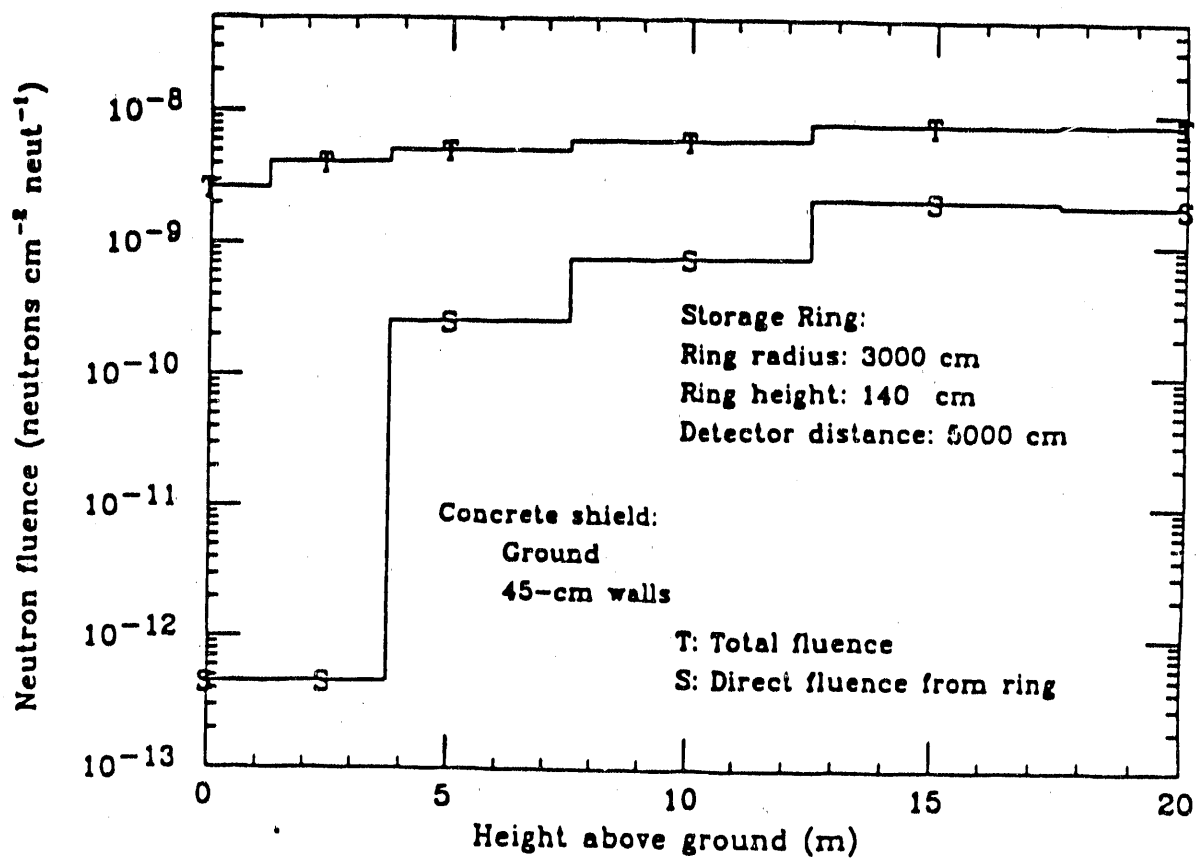


Figure 6.3. Neutron fluence as function of height above ground level (no roof).
Radius is set at 50 m.

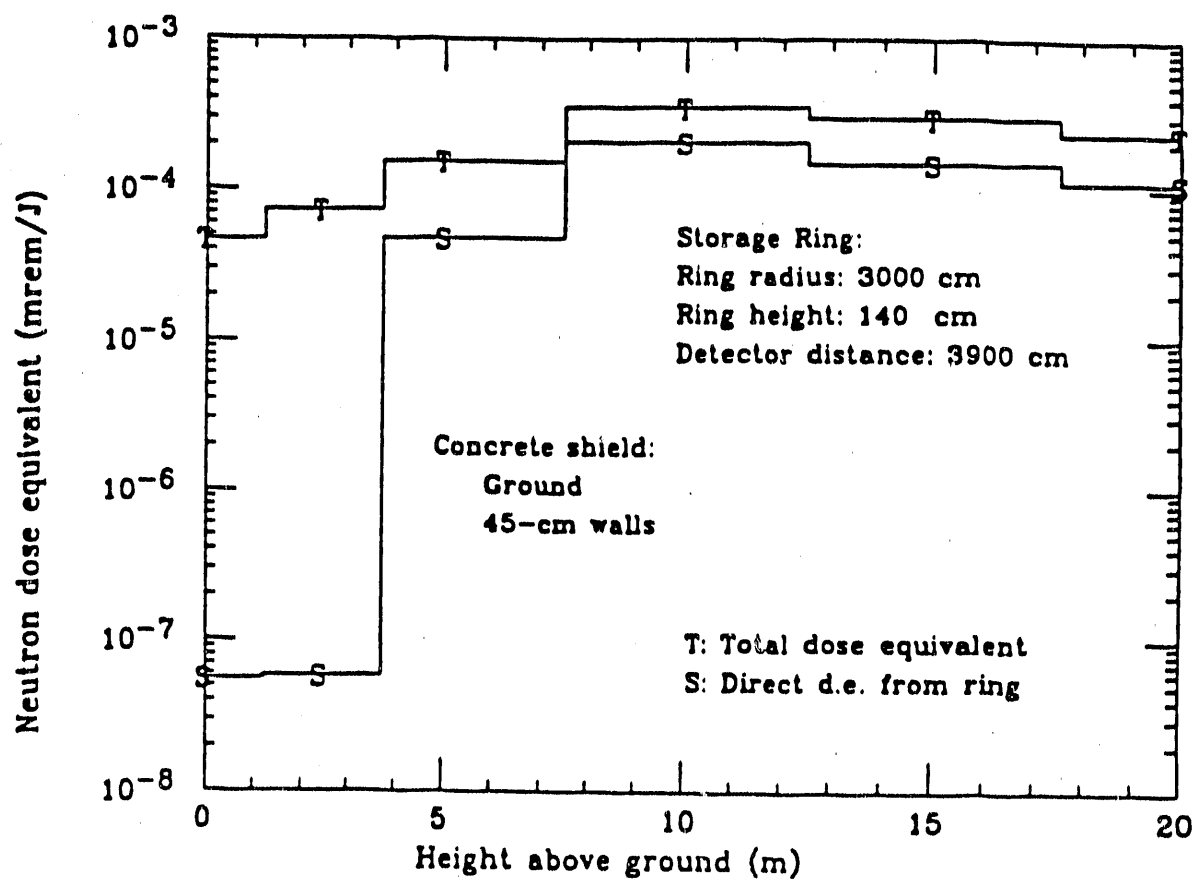


Figure 6.4. Neutron dose-equivalent as function of height (no roof). radius is set at 39 m.

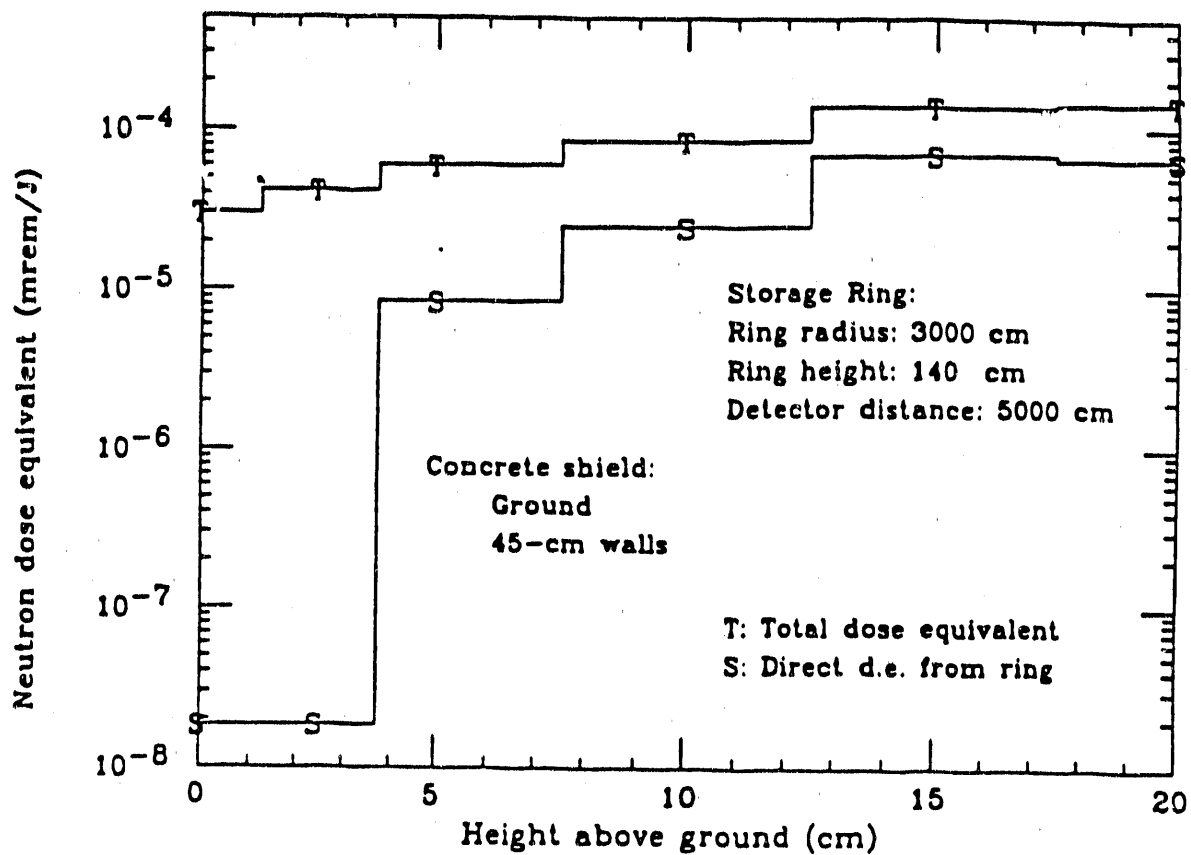


Figure 6.5. Neutron dose equivalent as function of height. radius is set at 50-m, no roof.

6.3 Neutron Spectra with no roof

As noted earlier the source spectrum assumed for the photoneutrons was a ^{252}Cf fission spectrum. Three different spectra are shown in figure 6.6. The distribution labeled with "S" is the basic photoneutron spectrum as used in the MORSE input. This spectrum is compared with spectra modified by scattering on materials such as air and concrete, the other two spectra labeled 1 and 4, seen by the detectors at the ring center and directly above the source respectively.

- With a concrete ground and two concrete walls but no roof, scattering from concrete contributes considerably to the softening of the spectrum.
- The spectrum "1" represents only air scattering, because of the line of sight concrete shielding. It is similar to spectrum "4" in the low energy range ($1\text{-}10^4$ eV), but due to the absence of direct source contribution the high energy ends of the spectra are not similar ($10^5\text{-}10^7$ eV).

Spectra calculated for the 5 detectors are illustrated in figures 6.7 and 6.8. They are all normalized to a source of one photoneutron production around the ring. The spectra are similar except where they are dominated by air-scattering. Figure 6.7 is the spectra in detectors within and above ring source, 0, and 30 m from the ring center. Figure 6.8 contains the spectra for the detectors outside of the ring source to a distance of 200 m away from the ring center (36, 90, and 200 m). Spectrum "A" (fig. 6.7), is the neutron spectrum at ring center. The spectrum is decreased uniformly within the energy range of $10^0\text{-}10^4$, compared to the spectrum "D" (exactly above the ring source). Figure 6.8, shows the neutron spectra outside of the ring source. As distance from the source increases, the value of the skyshine will decrease. This is evident from the detector responses of figures 6.7 and 6.8 (spectrum "K" has the lowest value compare to H, and E). Detector D shows the maximum response compared to the other detectors, because it is located directly above the beam.

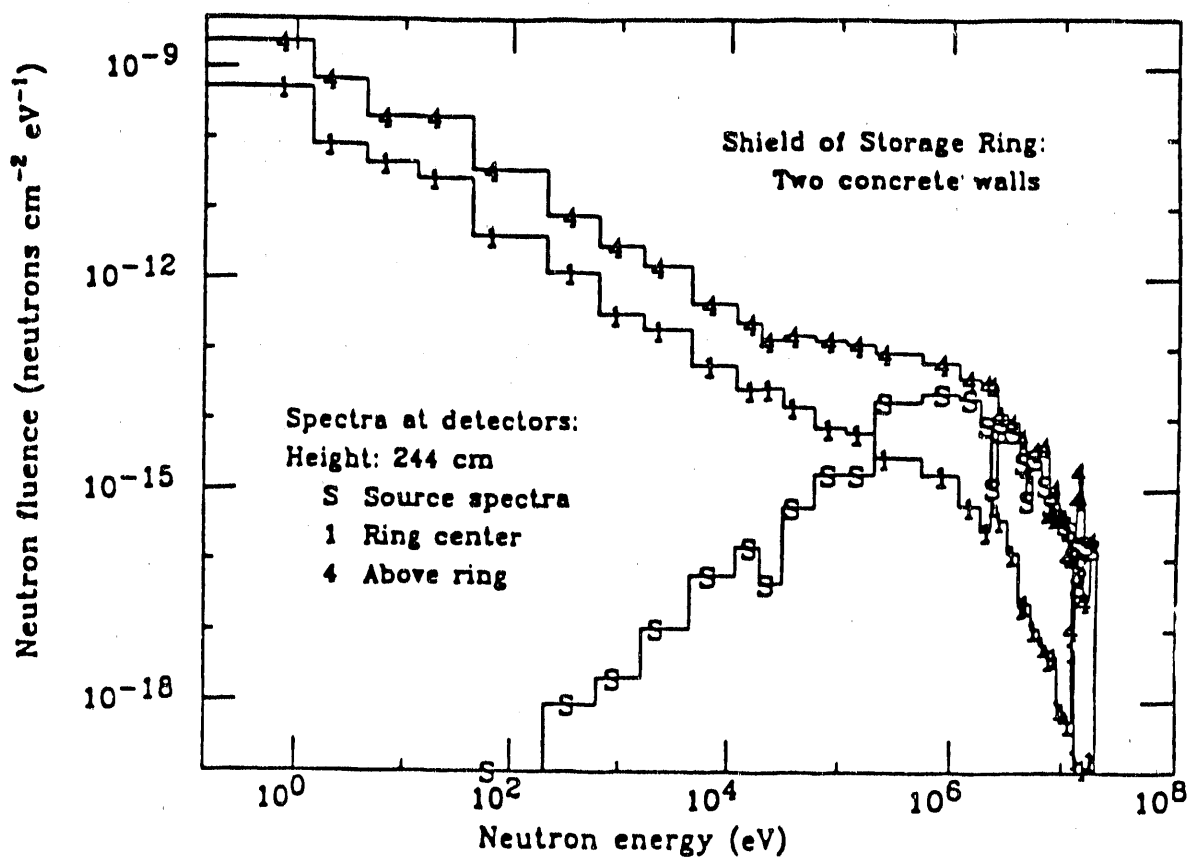


Figure 6.6, Comparison of source neutron spectrum (S), with spectra no roof at ring center (1), and directly above the source (4).

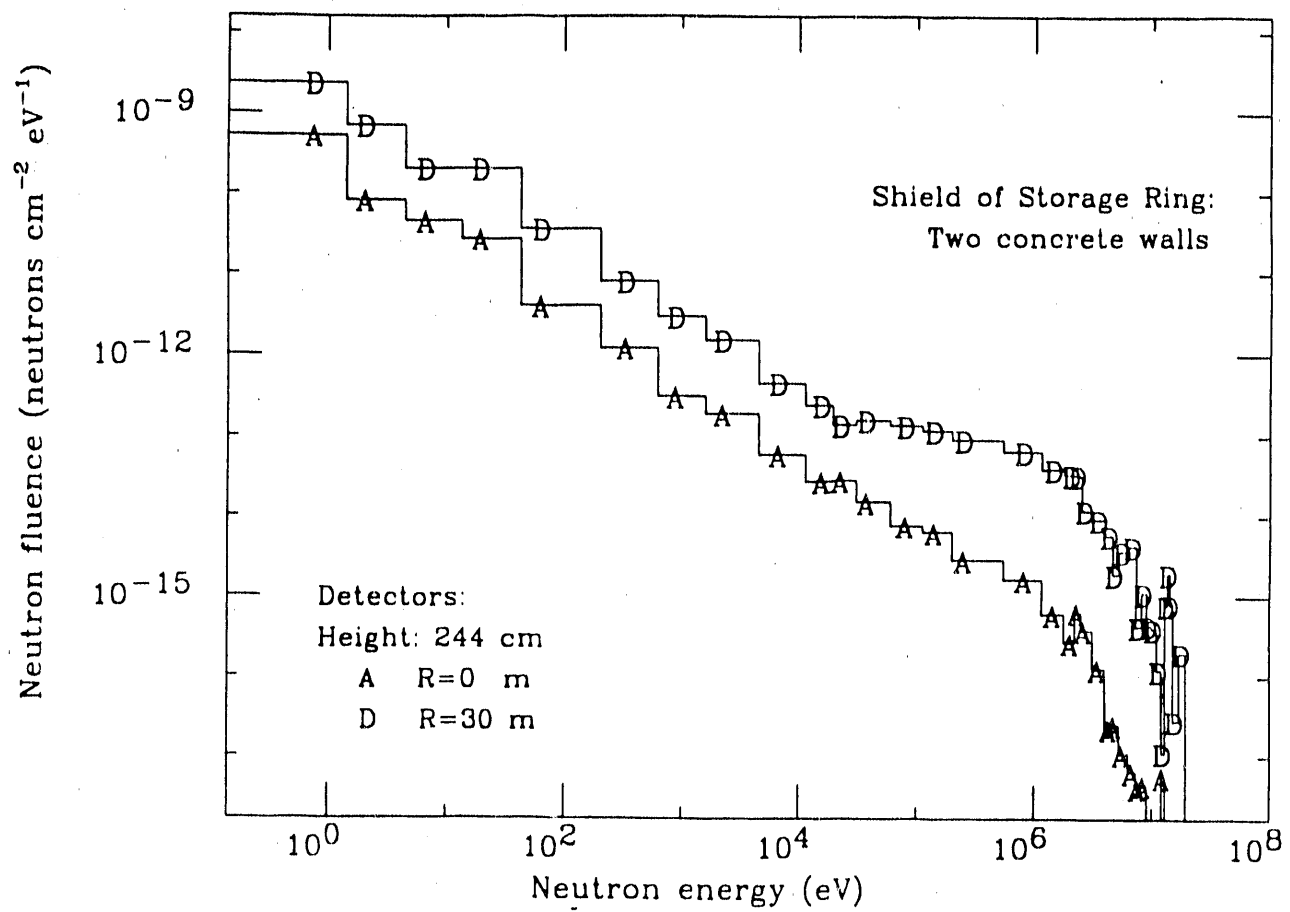


Figure 6.7. Neutron fluence spectra inside the ring (no roof).

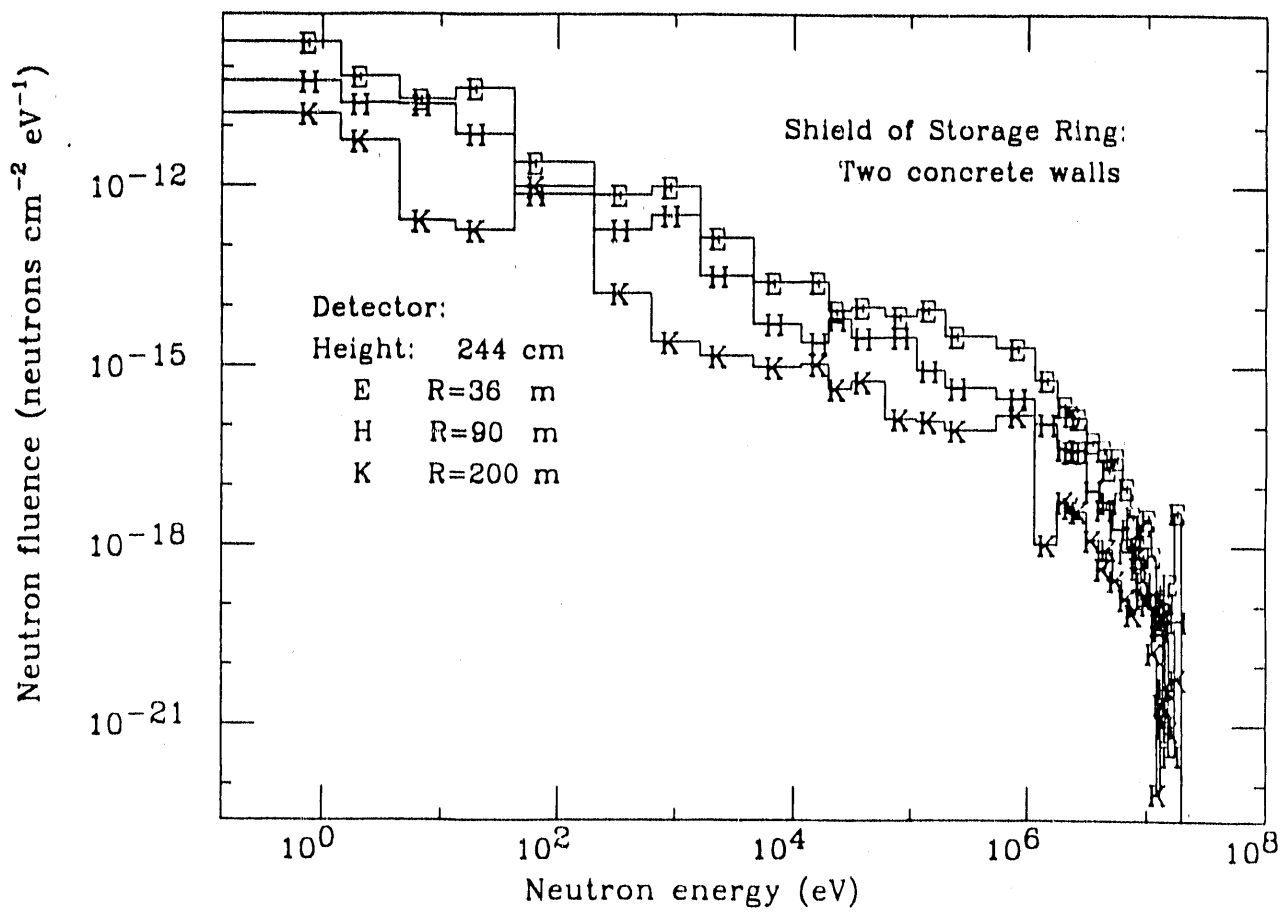


Figure 6.8, Neutron fluence spectra outside of the ring (no roof).

The skyshine spectra are dependent on the energy as E^{-x} , the value of x varies in different energy ranges. In the range of 10^0 - 10^5 eV, the value of x is almost equal to 1*. The value of x reduces to the range of 0.6-0.7 at energy level of 10^5 - 10^7 eV (figure 6.7 and 6.8).

- The value of x is about 0.6-0.7, at the larger distances (spectra "I" and "K") with the same energy range.

6.4 neutron dose and fluence with roof(radial)

Figure 6.9 shows the neutron fluence and dose equivalent as a function of radial distance from the Ring Source, with a 15, 30 and 45-cm roofs placed over the Storage Ring. These data show the effect of the various roofs placed over the source at a height of 244 cm covering the source between the two walls (tunnel geometry). The highest distribution is for no roof "0". A direct comparison of the roof effect is seen the area directly above the source (30 m from the ring center).

The maximum fluence is with no-roof above the source. The 15-cm thick roof reduces the direct fluence by about 95% (table 3). As it can be seen from the graph data "1", there is still a noticeable direct fluence that penetrates the 15-cm roof. No direct effect is observable for the two thicker roofs.

The fluence reduces as the distance from the source is increased (figure 6.9 indicates only total fluence, to be conservative the value of the direct fluence is not shown and the total fluence is treated as skyshine fluence). At 36 m from the ring center (4 m from the exterior wall), the 15-cm thick roof reduces the fluence by 82%. This reduction is more with 30-cm and 45-cm thick roofs (89% and 97% respectively). Between the distances of 50-70 m, the fluence is reduced more with the 30-cm and 45-cm thick roofs (90% and 97% respectively). Beyond the distance of 150 m from the ring source, the

* $x=1$ is similar to the slowing down process of the reactor neutrons.

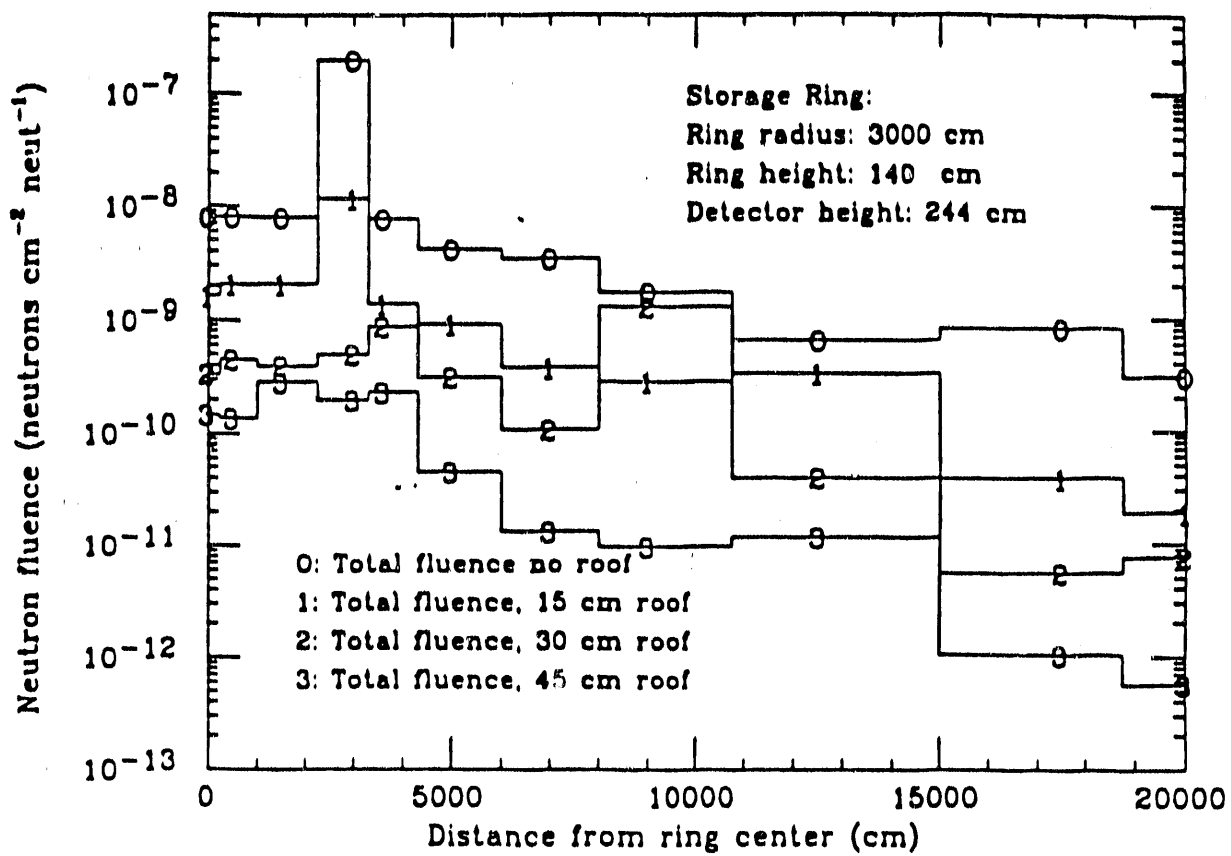


Figure 6.9, Neutron skyshine fluence as a function of distance from the ring center. Data are normalized to one photoneutron from the ring source. Detector heights are 244-cm except for 15-cm thick roof at 259-cm, 30-cm roof at 274-cm, and 45-cm roof at 289-cm.

fluence is reduced by more than 95% by the 15-cm thick roof and by more than 99% by the other two roofs.

Comparison of the 30-cm and 45-cm thick roofs shows, that the 45-cm thick roof, reduces the fluence by 25% at 4 m from the exterior wall, and 15% at the distance of 50-70 m. Figure 6.10 shows the dose equivalent with the same reduction pattern.

The results of the fluence calculations are tabulated (table 3) for the different locations in and around the ALS, for the different roof thicknesses for primitive comparison. The site boundary goes as far as 25 m down hill.

The dose-equivalent also shows the same reduction pattern as fluence.

Table 3. Calculated fluence (cm^{-2}) normalized to one uniform source neutron on Storage Ring.

Location	Distance from ring center (m)	Fluence (neutrons cm^{-2}) (*)			
		No roof	15-cm roof	30-cm roof	45-cm roof
Ring interior	0.25	8×10^{-9}	2×10^{-9}	4×10^{-10}	1.5×10^{-10}
Top of roof	30	2×10^{-7}	1×10^{-8}	1×10^{-9}	2×10^{-10}
Adjacent to outer wall	34	7×10^{-9}	1.5×10^{-9}	7×10^{-10}	2.3×10^{-10}
Mezzanine 1st floor (at 2.44)	39	7×10^{-9}	1.2×10^{-9}	5×10^{-10}	
	50	4×10^{-9}	1×10^{-9}	2.4×10^{-10}	
Mezzanine 2nd floor (at 5.0 m)	39	1×10^{-8}	1.6×10^{-9}	6.5×10^{-10}	
	50	5×10^{-9}	3×10^{-9}	4×10^{-10}	
Nearest site boundary at 25 m	104	7×10^{-10}	3×10^{-10}	4×10^{-11}	1×10^{-11}

(*) Spectral range included: Thermal 0.414 eV — 19.64 MeV.

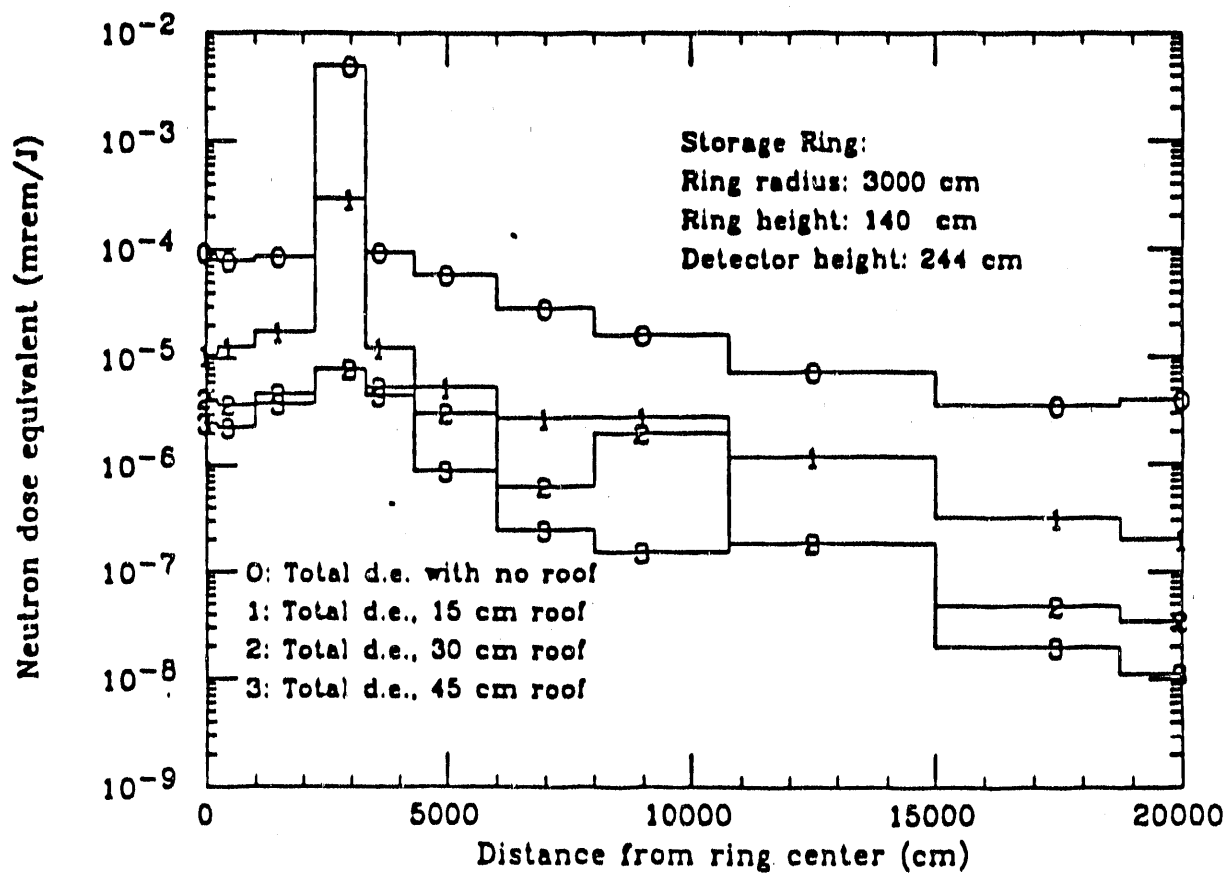


Figure 6.10. Corresponding neutron skyshine dose-equivalent as a function of distance from ring center.

6.5 dose and fluence with roof(altitude)

Figures 6.11 and 6.12 show the fluence as a function of height at nearby occupied areas (Mezzanine locations). The detectors are at radial distances from the source of 39 and 50 m. Three type of roof thicknesses are considered in this comparison (0, 15, 30 cm). The following observation can be made:

- At 39 m height (fig. 6.12), the total fluence contribution is reduced by an average of 80% from the ground level and up. This reduction averages more, with a 30-cm thick roof (by 94% of the total fluence of the no roof condition). From the ground level to about 7 m off the ground, the 30-cm thick roof reduces the total fluence 50% more than 15-cm thick roof. This reduction of fluence increases from 7 to 20 m off the ground which ultimately results in the reduction of skyshine fluence. For no-roof, if the ring portions are visible (above a wall height of 244 cm), direct fluence contributions range 20-50% (39 m fig 6.12, T and S).
- At 50 m height (fig. 6.11), the total contribution of the fluence (no roof) reduces by 47% from the total fluence of the 39 m height. Comparing the total fluence of the two roofs, 30-cm thick roof reduces the total fluence by a larger factor than the fluence from the 39 m height. At 50 m figure 6.11, direct fluence is less, about 10-20%. Direct fluence is expected to decrease with radial distance in comparison to total fluence. With either roof the direct fluence is the same between ground level to a highest of 7 m off the ground. The direct contribution is not significant at any height.

Figures 6.13 and 6.14 show the dose equivalent as functions of height at 39 and 50 m radial distances. The dose equivalent results in the locations are summarized in table 4. The results are normalized to beam loss of 2×10^6 joules/year.

Table 4. Dose-equivalent rates at distances of important locations, normalized to 2×10^6 J beam loss.

Location	Distance from ring center (m)	Annual dose equivalent (mrem/year)(*)			
		No roof	15-cm roof	30-cm roof	45-cm
Ring interior	0-25	160-180	20-30	7-10	5-8
Top of roof	30	10,000	600	16	14
Adjacent to outer wall	34	260	34	12	8
Mezzanine 1st floor (at 2.44 m)	39	150	17	11	
	50	84	10	3	
Mezzanine 2nd floor (at 5.0 m)	39	300	30	13	
	50	120	16	5	
Nearest site boundary	104	36	6	4	0.3

(*) Spectral range included: Thermal 0.414 eV — 19.64 MeV.

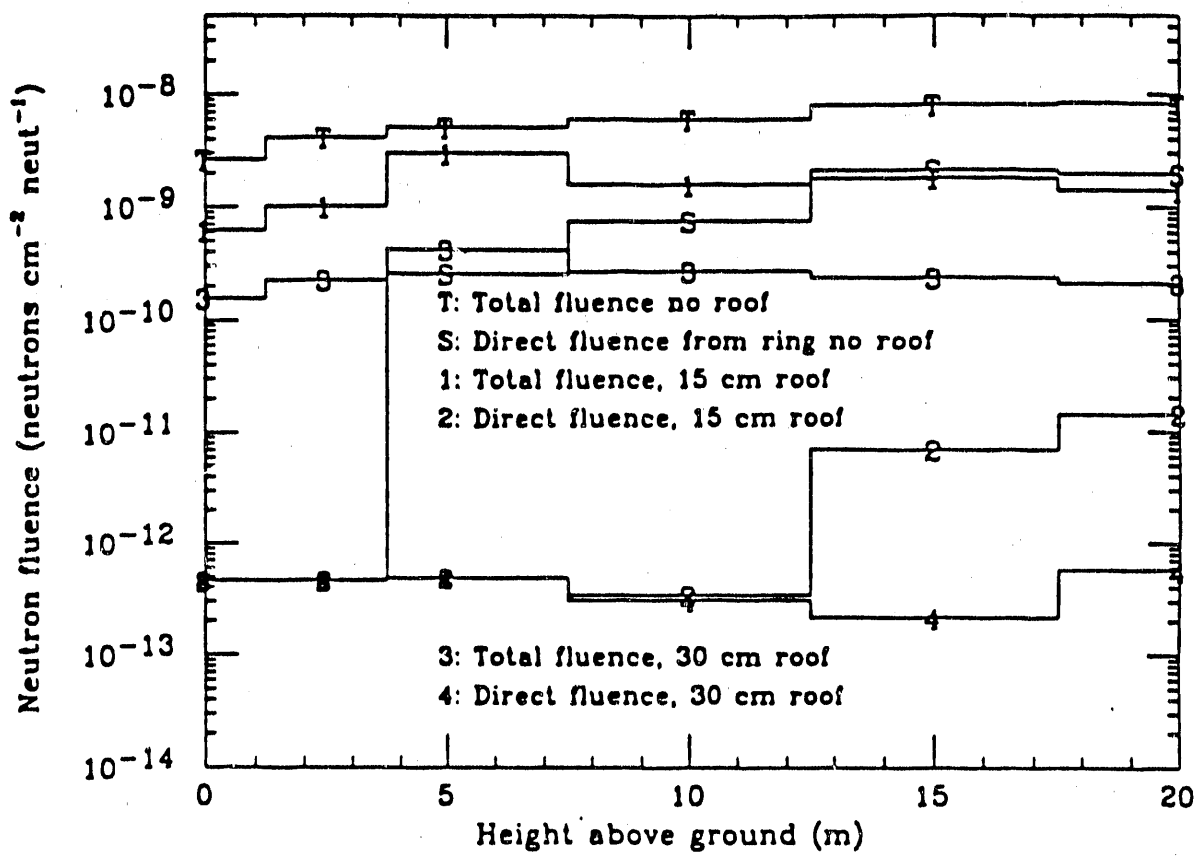


Figure 6.11, Neutron fluence as a function of height at mezzanine locations. Normalized to uniform ring source of 1 neutron. Detector arrays are set at 50-m.

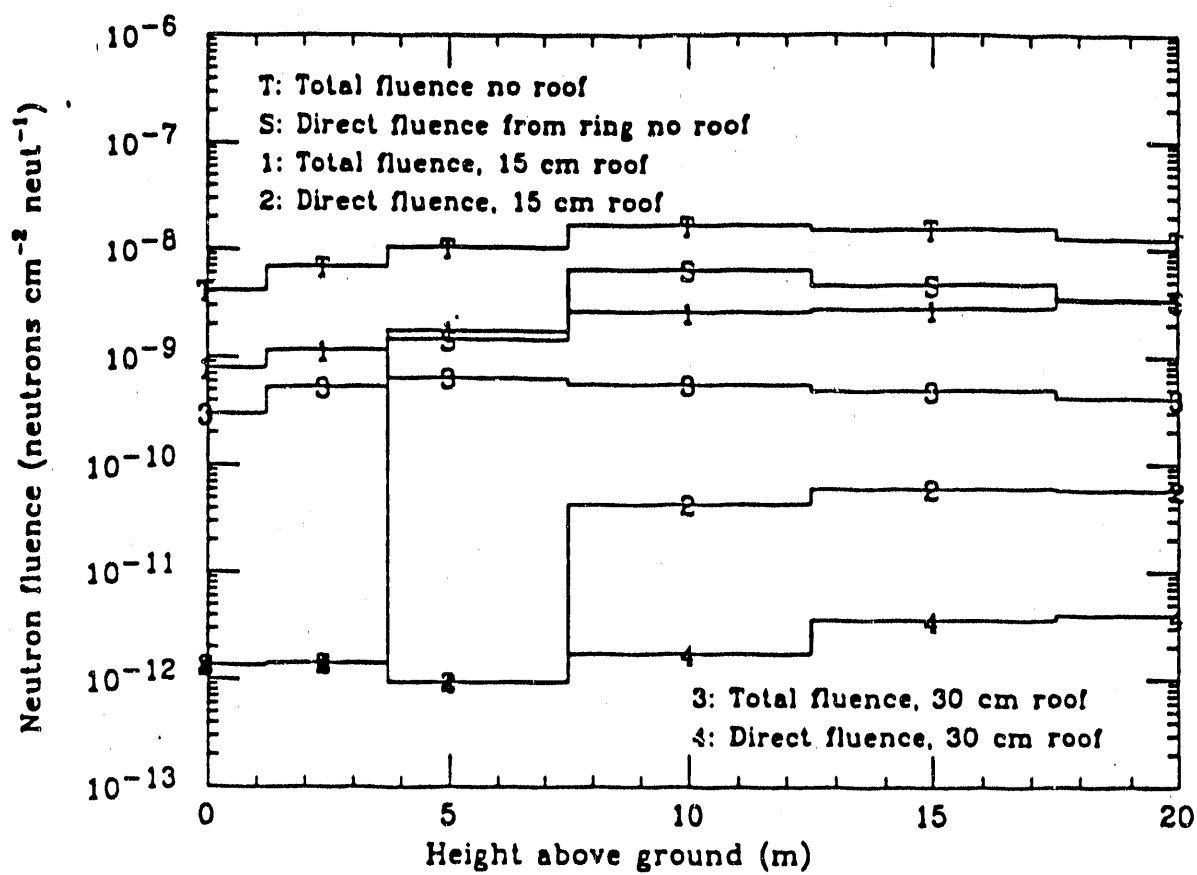


Figure 6.12, Neutron fluence as a function of height at mezzanine locations. detector arrays set at 39-m.

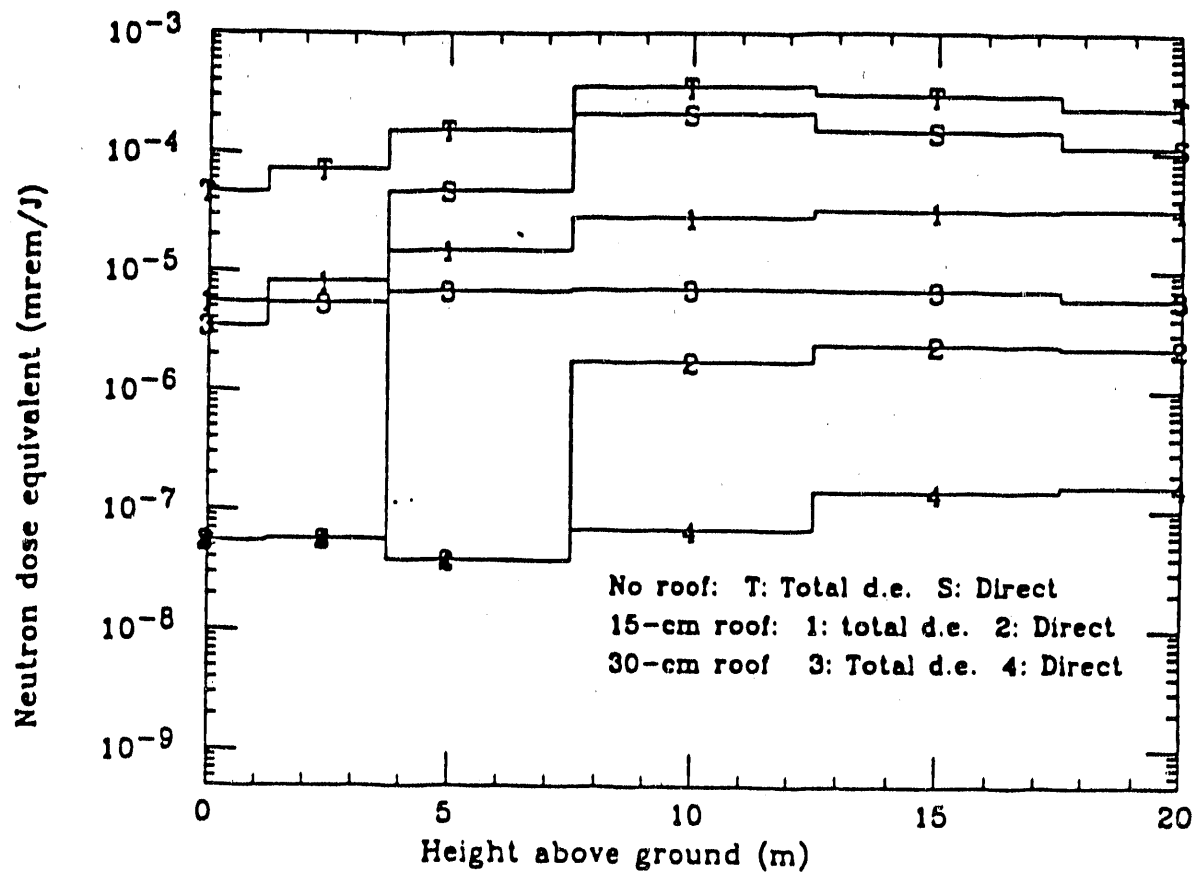


Figure 6.13, Neutron dose-equivalent as a function of height at mezzanine locations. Normalized to uniform electron beam loss at 1×10^6 J/year. Detector arrays set at 39-m.

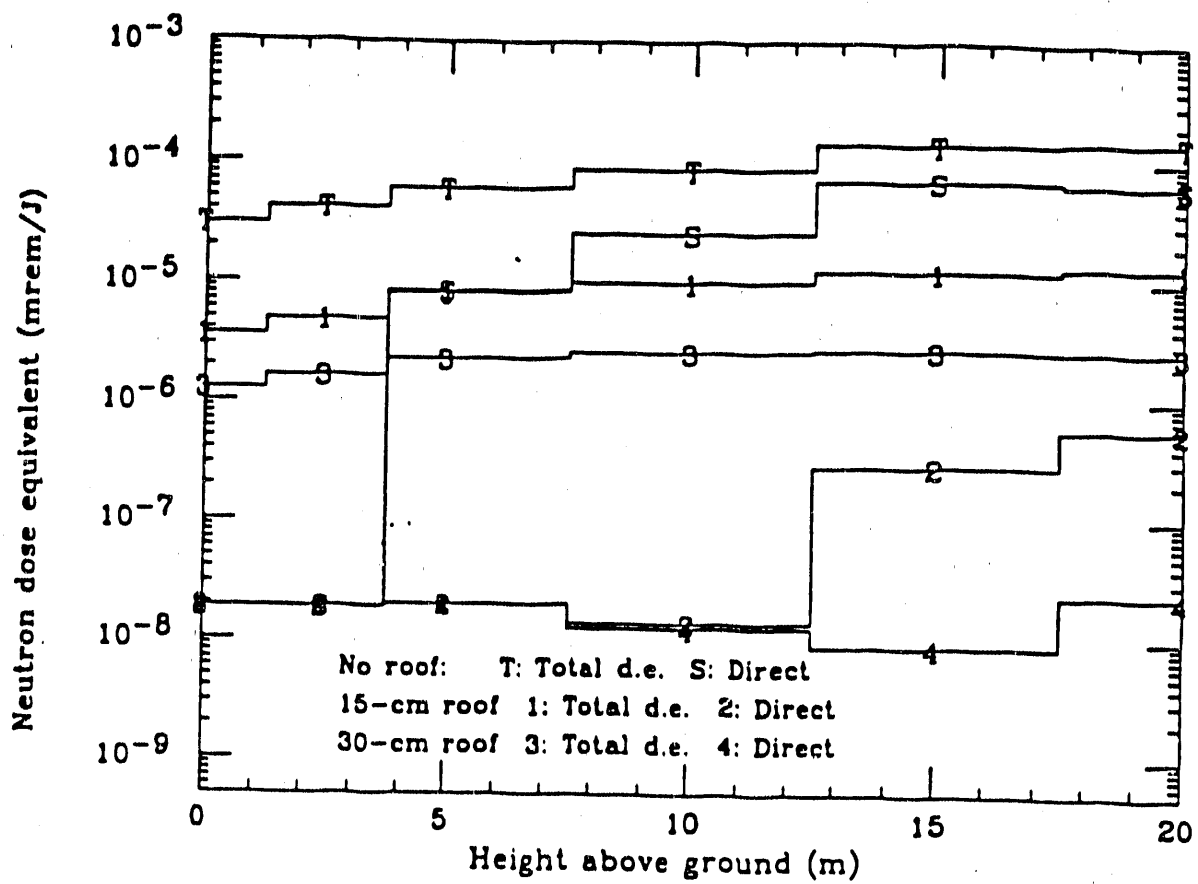


Figure 6.14, Neutron Dose equivalent at mezzanine location. Detector arrays set at 50-m.

7.0 Comparison of MORSE shielding calculations with analytical models

7.1 Shielding Calculations

- giant resonance (GR).

For neutron energy of less than 20 MeV, the neutron dose equivalent is given by the following equation (ref. 3), based on a 15 GeV electron beam striking an iron target (the Stanford positron-electron project-PEP-):

$$DE(GR) = 122.4E_0 \left(\frac{\cos\theta}{a+d} \right)^2 Z^{0.73} \exp\left(\frac{-d\rho \sec\theta}{\lambda_2} \right) * \text{mrem/J} \quad (7.1)$$

Figure 7.1, was obtained by numerical integration along the ring source, using equation 7.1. The circumference of the ring source was divided into 500 equal segments over 360° .

Parameters of the equation 7.1 are as follows:

E_0 beam energy loss in a target in GeV.

θ angle from target to measurement point.

d shield thickness in cm.

a target to shield distance cm.

λ_2 removal mean-free path, for concrete = 30 g/cm^2 .

ρ shield density, g/cm^3 .

Z atomic number of target (for Iron this value is 26).

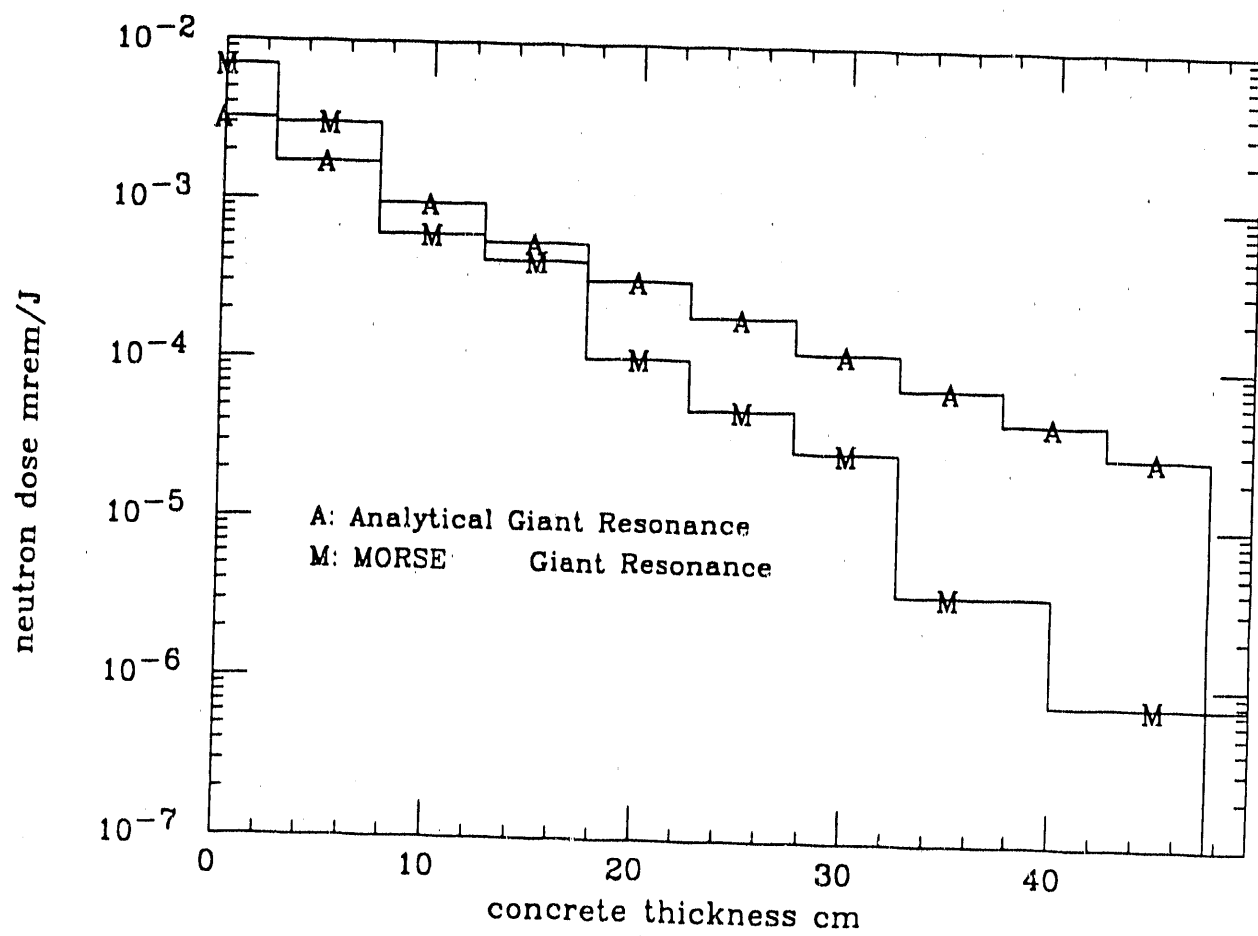


Figure 7.1, Comparison of analytical and MORSE giant resonance.

7.1.1 MORSE in shielding

In using the MORSE code for shielding, the whole ring source was modeled like the skyshine problem. But the arrangement of the detectors was different according to the concrete thickness. In the first run 7 concrete wall thicknesses were chosen. The detectors were placed along the x-axis at the height of 140.0 cm off the ground to see the source directly. The result of the calculations are plotted on fig. 7.1. The second MORSE run was done to compare the dose at the surface of a 45-cm thick wall. The results are shown on figure 7.2 and are comparable with the figure 7.1.

7.1.2 COMPARISON OF ANALYTICAL CALCULATIONS WITH MORSE

From figure 7.1, the giant resonance dose from the MORSE and analytical calculations are very close and are different by an average factor of 2 (0 to 15-cm thickness). But MORSE results diverge more as the thickness is increased. the MORSE dose with a 45-cm thick wall is 20 times less than the analytical result.

According to ref. 3 the measurement of neutron fluences and dose equivalents from a 15 GeV electron beam striking an iron target, and a comparison of analytic-empirical calculations with MORSE, shows that "the MORSE code is able to predict both neutron and photon dose equivalent for geometries where the shield is relatively thin, but fails as the shield thickness is increased". The dose is underestimated by MORSE at larger thicknesses (Ref. 19). That discrepancy is consistent with the results shown in figure 7.1. A significant contribution of a high energy neutron component to the measured fluence would give this type of difference between empirical and MORSE results.

7.2 Comparison of the approximate skyshine calculation with MORSE

For the purpose of comparison of values obtained by the equations 2.7 and 2.8 and MORSE skyshine, an observation point at the same level as the source, 140 cm off the ground, and 9 m away from the source (39 m from the ring center) along the x-axis was

considered.

The solid angle subtended by the shielding wall perimeter was estimated to be $\Omega=1.4\pi$ Str. Then the ring source was divided into 10 degree intervals. Using equations 2.7 and 2.8 the total value for the skyshine fluence was calculated to be;

$$\phi_{\text{sd}} = 4.8 \times 10^{-8} \text{ n/cm}^{-2}\text{-n}$$

The same point was calculated using MORSE. Only one detector was placed at the point of the observation. A batch of 1000 neutrons was followed to obtain the skyshine fluence. The fluence value read from the detector was:

$$\phi = 9.8 \times 10^{-9} \text{ n/cm}^{-2}\text{-n}$$

Comparing the NCRP value with the skyshine dose value of MORSE, there is some variation between the two values. The more elaborate and more exact MORSE predicts a factor of 5 smaller skyshine dose than the simple approximation.

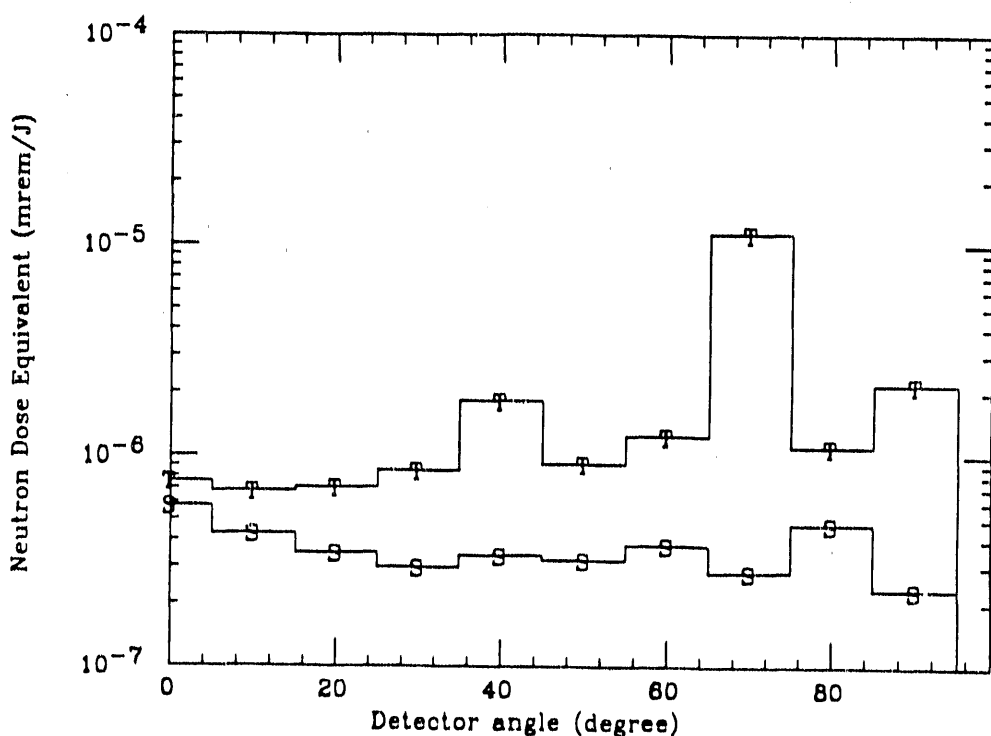


Figure 7.2. Neutron dose equivalent vs. detectors angle at the surface of a 45-cm concrete wall.

8.0 SUMMARY AND CONCLUSIONS

This simplest use of MORSE was used to gain experience and confidence in physically reliable results. Point detectors and simple, convenient preliminary checks were made against vacuum geometry only and with air introduced as the first and only medium. In the run with only vacuum present, a fundamental fluence test was made by comparison of simple geometry: $\phi = 1 / (4\pi r^2)$, where r is the total detector distance. The second run was made only with air, and illustrated sky-transport. The distribution was similar but increased generally.

In comparison tests with boundary crossing estimates, consistency was found. Fluence and dose-equivalent studies agreed and ensured that geometry and detector usage was correctly formulated.

Simple test runs made with impervium wall materials were made to compare with first results where real concrete was installed. These results were comparable and found increase in the effect of concrete shielding. For useful production runs presented here, 10,000 photoneutron source neutrons were generated.

Some interactions physically available to transported neutrons, are not relevant in the present problem, interactions such as fission events, and neutron-capture gamma generation. Russian roulette, spectral or transport cuts or biases, that are part of MORSE structure, were not tried in any of the runs. The entire generated spectrum was transported by simplest MORSE options and thermal neutrons were included in the fluence and dose-equivalent results.

In some of the later runs, due to the scattering of the roof, the time to process each batch was almost four times longer than the time to process the previous batches, which made a significant difference in CP'J time. There were two point-detector arrangements chosen to test the skyshine for two different runs. The first set of detectors was arranged as a function of distance from the ring source to 200 m, and two second arrangements provided as functions of height at $R = 39$ and 50 m. The second set was useful to see the

skyshine variation in second floor Mezzanines.

The basic photoneutron source for the Storage Ring occurs when an 1.9-GeV electron initiates an electromagnetic cascade (EM) and exhausts all energy available. The photon spectrum generated within this cascade produces virtually all reactions leading to photoneutrons. Each EM cascade must begin in the stainless steel beam pipe but unpredictable energy escapes. The most natural material is then the iron of beam-magnet elements. The choice of iron is conservative. The photoneutron source spectrum adopted was the californium fission spectrum.

The assumption made was a uniform beam loss in the ring. In reality, the losses will be "lumpy" instead, and this pattern cannot be predictable. This situation can have advantages because the "uniform" rates would average less and the point locations can be covered by small, local neutron shielding such as polyethylene slabs.

The actual engineering design was started with hand calculations of shielding needs for walls and roofs and resulted in the wall- and roof-choices of 4.5 and 30 cm, respectively. Construction needs are obviously not just for radiation protection but for engineering and seismic stability. Results of the Monte-Carlo study confirm that basic shielding needs are fully adequate; the average dose-equivalent closest to the Storage Ring with a 30-cm roof is about 12 mrem/year to protect the many workers and visitors in proximity to experimental beams and nearest buildings.

The site-boundary dose equivalents are important. At the nearest site boundary, 15 and 30-cm roofs show small difference of dose equivalent (6 and 4 mrem/year) with, the 30-cm thick roof being, of course, better, is more adequate.

In conclusion, the Monte-Carlo calculation results confirm the adequacy of the planned shielding for skyshine.

9.0 REFERENCES

1. M.B. Emmett, "the *MORSE monte carlo radiation transport code system*" Oak Ridge National Laboratory, Oak Ridge, TN, Report ORNL-4972 (February 1975).
2. ICRP73, 1973, "Data for protection against Ionizing Radiation from External Sources:supplement to ICRP publication 15." ICRP Publication No.21(Oxford:Pergamon Press,1973).
3. T.M. Jenkins," Neutron and Photon Measurements Through Concrete From a 15 GeV Beam on a Target",Stanford Linear Accelerator, Stanford, California, 1978.
4. NCRP77, "Radiation Protection Design Guidelines for 0.1 - 100 MeV particle Accelerator Facilities." Report No. 51, Washington D.C.(1977).
5. RSIC Data Library Collection; FEWG1;37 neutron, 21 Gamma Ray coupled, P_3 , Multigroup library in ANISN format, Oak Ridge National Laboratory, Radiation Shielding Information Center(1979).
6. "RSIC computer code collection:MORSE-CG, general Purpose Monte Carlo Multigroup Neutron and Gamma-Ray with Combinatorial Geometry.";Radiation Shielding Information Center, Oak Ridge, TN,RSIC report No. CCC-203C&D (1984).
7. W.P. Swanson , "calculation of Neutron Yield Released by Electron Incident on Selected Materials."Health Physics 35,353-367 (1978).
8. W.P. Swanson,"Improved Calculation of Photoneutron Yield Released by Incident Electrons."Health Physics 37,347-358 (1978).
9. W.P Swanson, "Implementation of the ORNL Program MORSE; Preliminary calculation of Neutron Skyshine Near the LBL Advance Light Source." Lawrence Berkeley Laboratory (1988).

10. M.S. Zisman, Information on Beam losses Provided in Private Communication, Lawrence Berkeley Laboratory (1978).
11. W.P. Swanson, Neutron Dose Equivalent at Electron Storage Rings, Lawrence Berkeley Laboratory (1985).
12. W.P. Swanson, Minimum Concrete Requirement For ALS, LBL Report, Lawrence Berkeley Laboratory (1988).
13. J.D. Jackson, Classical Electrodynamics, John Wiley and Sons, Inc.(1962).
14. LBL Report, an ALS handbook a summary of the capabilities and characteristic of the Advance Light Source, Lawrence Berkeley Laboratory (1989).
15. PUB-5172 Rev., 1-2 GeV SYNCHROTRON RADIATION SOURCE, conceptual design report, Lawrence Berkeley Laboratory (July 1986).
16. W. R. Nelson, PROPERTIES OF THE EM CASCADE, Stanford Linear Accelerator, (Feb. 1987).
17. W.P. Swanson, RADIOLOGICAL SAFETY ASPECTS OF THE OPERATION OF LINEAR ACCELERATORS, International Atomic energy Agency, VIENNA, 1979.
18. W.P. Swanson, Deluca, otte, Schilthem, ALADDIN UPGRADE DESIGN STUDY: SHIELDING, Lawrence Berkeley Lab, department of medical physics (University of Wisconsin), Synchrotron Radiation Center (Stoughton WI.), April 23 1985.
19. T.M. Jenkins, Stanford Linear Accelerator (Private Communication 1989).
20. T.M. Jenkins, Stanford Linear Accelerator (Private Communication 1990).

APPENDICES

A1.0 MORSE STRUCTURE

MORSE code is a large general-purpose multigroup Monte-Carlo radiation transport computer code system that has been undergoing development at Oakridge National Lab. since the late 1960. It calculates the transport of uncharged particles (neutron and/or gamma rays). MORSE has been more widely used than any other Monte-carlo radiation transport code available. The principal reason for this popularity is that the code is relatively easy to use, it is independent of any large installation or distribution center. There are many features associated with this code such as:

1. Applicable to multiplying or non-multiplying media
2. Can operate in a fixed source
3. Uses cross_section and/or albedo
4. Treats regular and/or delta scattering
5. Has a two-and three-dimensional geometry picture drawing capability
6. Uses ANISN library multigroup cross_section and anisotropic scattering formats, including upscatter for any number of thermal energy group.
7. Can create separate Klein-Nishina, pair-production, and photoelectric reaction for gamma ray next event estimation.
8. Accepts user written routines, and many more features.

A1.1 ROUTINES

It is by the use of the user-written routines that the MORSE is very flexible. Most of the effort is made toward the description of source and estimation of process. User routines can be used to call other routines, and any information regarding to any part can be obtained and printed out.

A1.1.1 Main Routine

The main routine performs the following functions:

1. set a size for blank common, the blank common is the regional size needed.
2. puts the labeled commons in specific order of use.
3. assigns a junk word for every system which has to be loaded. finally, it calls the MORSE subroutine to do the actual processing of the job of a scattering and collision of particles.

This routine is formed by several common blocks. The primary common is NUTRON, and its variables are discussed below:

1. NAME: each particle is given a unique name, including an integer (these particle parameters are stored in an area of blank common called the "Neutron bank". They are processed in order of the largest numbers. Most of the parameters in NUTRON common given to the new particles are the same as old particles. Primary and secondary particles are distinguished by energy group).
2. NAMEX: if a particle is generated by *splitting, fission neutrons or neutrons produced gamma rays* will have a different name (assigned a different integer). This is called the particle's family name.
3. IG: current energy group

4. IGO: previous energy group
- 5) NMED: particles are considered in different media (air and concrete) NMED is the identification number for the current location.
- 6) MEDOLD: medium number at previous location
- 7) NREG: region number at current location.
- 8) U,V,W: new direction cosines
- 9) UOLD,VOLD,WOLD: old direction cosines
- 10) X,Y,Z: new location of a particle
- 11) XOLD,YOLD,ZOLD: old location of a particle
- 12) WATE: current weight, the value of WATE is initially set.
- 13) WTBC: weight just before current collision
- 14) IBLZN: current zone number
- 15) IBLZO: old zone number
- 16) AGE: current age
- 17) OLDAGE: previous age

A1.1.2 Physical analogies corresponding to MORSE weights

The physical analogies corresponding to MORSE weight has been in different events. WTBC has to be used for pre-collision analysis, since MORSE calls the collision analysis routine after the collision. Reference 6 includes all these analogies which include, *current, J; flux, ϕ ; collision density, $\Sigma_i \phi$; fission neutron production, $v \Sigma_f \phi$; and etc.*

A1.1.3 MORSE (NFLT)

MORSE is the routine which does the walk process and controls other events that comprise the Monte-Carlo process. The problem is assumed to consist of a number of runs (specified by *NQUIT* in the input file), each one containing a number of batches (NITS), and each batch with a number of source particles (NSTRT). Then the function of MORSE is broken down into nested loops with inner loops consisting of execution of walk process for each particle. The next loop is for each batch of particles and the outer loop is for each run.

Most of these values are inserted in data files such as termination of history and bookkeeping of pre-collision parameters. It is also possible to set a time limit to terminate a problem after a certain elapsed time. There are some options in MORSE each identified by a number corresponding to an event. The variables are, **NDEAD(I)**, and **DEADWT(I)**. Depending upon the value of I, MORSE can perform several events for example;

I=1 Russian Roulette kill of a particle

I=2 Particle escaped the system

I=3 Particle reaches energy cut off

I=4 particle reaches age limit (retired)

Another variable in MORSE is "NPSCL(I)", keeps track of the number of the various interaction and termination types for example:

I=5 Number of real collisions

I=6 Number of albedo collisions

I=9 Number of energy deaths

I=10 Number of age terminations

Setting I=0, MORSE discards all the above events and collisions and they will appear as zero in the output.

A1.1.4 Subroutine BANKR(NBNKID)

BANKR has been modified to give boundary crossing estimator. Noticing after the common blocks, there are data provided to perform boundary_crossing estimates. There are many subroutines within BANKR. The particular subroutines are called for analyzing an event by determining the index "NBNKID". In most problems;

NBNKID=-4 calls NRUN (end of run)

NBNKID=-3 calls NBATCH (end of batch)

NBNKID=-2 calls STBTCH (start new run)

NBNKID=-1 calls STRUN and HELP

BANKR is called with as many as 17 values of the argument (NBNKID) to direct the analysis. A complete list is indicated in card BANK 280. The NBNKID=7, calls the BDRYX, which is the boundary crossing estimator. In order to do the estimation, statements between card 420 and 450 are accessed when NBNKID=7. This is the boundary_crossing event. The loop at BANK 90 to 110 calculates the area of boundary estimates (AREA(IZON)), and the 33 statements between card BANK 190 and 200, print out the results of boundary_crossing estimates.

The statements from line 7 to line 70, first test the coordinate Z, to be close to a boundary at a height of detector (DEHTH), and then determines the new zone (IZON). Other values relevant to boundary_crossing events are, SKYSUM, SKYNUM, and SKYWATE.

SKYSUM, contains the sum of WATE/(CCOSINE*AREA).

SKYSUM, contains a simple, unweighted count of neutron events at boundary IZON

SKYWATE, contain the sum of neutron weights, WATE

At the end the subroutine FLUXST is called to do separate analysis to check the boundary_crossing calculations produced in BANKR.

SUBROUTINE BANKR(NBNKID)

BANK 10

C THIS VERSION IS FOR POINT DETECTORS ONLY; IT CALLS SDATA
 C AT STMT 1 AND RELCOL AT STMT 5.

C DO NOT CALL EUCLID FROM BANKR(7)

BANK 20

COMMON /APOLLO/ AGSTRT, DDF, DEADWT(5), ETA, ETATH, ETAUSD, UINP, VINP, BANK 30
 1 WINP, WTSTRT, XSTRT, YSTRT, ZSTRT, TCUT, XTRA(10), BANK 31
 2 IO, I1, MEDIA, IADJM, ISBIAS, ISOUR, ITERS, ITIME, ITSTR, LOCWTS, LOCFWL, BANK 32
 3 LOCEPR, LOCNSC, LOCFSN, MAXGP, MAXTIM, MEDALB, MGPREG, MXREG, NALB, BANK 33
 4 NDEAD(5), NEWNM, NGEOM, NGPQT1, NGPQT2, NGPQT3, NGPQTG, NGPQTN, NITS, BANK 34
 5 NKCALC, NKill, NLAST, NMEM, NMGP, NMOST, NMTG, NOLEAK, NORMF, NPAST, BANK 35
 6 NPSCL(13), NQUIT, NSIGL, NSOUR, NSPLT, NSTRT, NXTRA(10) BANK 36
 COMMON /NUTRON/ NAME, NAMEX, IG, IGO, NMED, MEDOLD, NREG, U, V, W, UOLD, VOLDBANK 40
 1 , WOLD, X, Y, Z, XOLD, YOLD, ZOLD, WATE, OLDWT, WTBC, BLZNT, BLZON, AGE, OLDAGEBANK 41
 integer blznt, blzon
 COMMON/USER/AGSTRT1, WTSTRT1, XSTRT1, YSTRT1, ZSTRT1,
 1 DFF1, EBOTN1, EBOTG1, TCUT1, IO1, I11

NBNK = NBNKID

BANK 50

C NBNK = -4 MEANS: (104) CALL NRUN (END OF RUN)
 C NBNK = -3 MEANS: (103) END OF BATCH
 C NBNK = -2 MEANS: (102) START NEW RUN, SAME INPUT (RARELY USED)
 C NBNK = -1 MEANS: (101) START NEW RUN
 C NBNK = 0 MEANS: (101) START NEW RUN

IF (NBNK) 100,100,140
 100 NBNK = NBNK + 5
 GO TO (104,103,102,101), NBNK

BANK 60

BANK 70

BANK 80

C START OF NEW RUN
 101 CALL STRUN
 RETURN

BANK 90

BANK 110

C START NEW BATCH
 102 NBAT = NITS - ITERS
 NSAVE = NMEM
 CALL STBTCH(NBAT)
 C NBAT IS THE CURRENT BATCH NO. LESS ONE
 RETURN

BANK 120

BANK 130

BANK 140

BANK 150

BANK 160

C END OF BATCH
 103 NSAVE = NSTRT
 CALL NBATCH(NSAVE)
 C NSAVE: NO. OF PARTICLES STARTED IN THE BATCH JUST COMPLETED
 RETURN
 104 CONTINUE

BANK 170

BANK 180

BANK 190

C CALL NRUN(NITS, NQUIT)
 C NITS IS THE NO. OF BATCHES COMPLETED IN THE RUN JUST COMPLETED
 C NQUIT .GT. 1 IF MORE RUNS REMAIN
 C .EQ. 1 IF THE LAST SCHEDULED RUN HAS BEEN COMPLETED
 C IS THE NEGATIVE OF THE NO. OF COMPLETE RUNS, WHEN AN
 C EXECUTION TIME KILL OCCURS
 RETURN

BANK 200

BANK 210

BANK 220

BANK 230

BANK 240

BANK 250

BANK 260

140 GO TO (1,2,3,4,5,6,7,8,9,10,11,12,13), NBNK
 C NBNKID COLL TYPE BANKR CALL NBNKID COLL TYPE BANKR CALL BANK
 C 1 SOURCE YES (MSOUR) 2 SPLIT NO (TESTW) BANK 290
 C 3 FISSION YES (FPROB) 4 GAMGEN YES (GSTOREBANK 300
 C 5 REAL COLL YES (MORSE) 6 ALBEDO YES (MORSE) BANK 310
 C 7 BDRYX YES (NXTCOL) 8 ESCAPE YES (NXTCOLBANK 320
 C 9 E-CUT NO (MORSE) 10 TIME KILL NO (MORSE) BANK 330

C	11	R R KILL	NO (TESTW)	12	R R SURV	NO (TESTW)	BANK 340
C	13	GAMLOST	NO (GSTORE)				BANK 350
1	CONTINUE						BANK 360
	CALL SDATA						
	RETURN						BANK 370
2	RETURN						BANK 380
3	RETURN						BANK 390
4	CONTINUE						BANK 400
	RETURN						
5	CONTINUE						BANK 410
	CALL RELCOL						
	RETURN						
6	RETURN						BANK 420
7	CONTINUE						
	RETURN						
8	RETURN						BANK 450
9	RETURN						BANK 460
10	RETURN						BANK 470
11	RETURN						BANK 480
12	RETURN						BANK 490
13	RETURN						BANK 500
	END						BANK 510

A1.1.5 Subroutine SOURCE

This subroutine determines the initial parameters for all primary particles. There are number of variables used to input the source particles. The variables which are changed are as follows:

WATE: particle source weight

IG: Particle energy group

NWT: location of group zero source probability

The values required for this subroutine are;

ISOUR: determines the type of the source, done in input

NPGQT3: total number of groups over which the problem is defined.

DDF: starting weight, corrected for source by defining over different number of groups.

NMTG: total number of groups.

The parameters in this subroutine define a ring source, and at the top after defining some commons, the radius of the ring is inputed. All the lines prior to line 30, define a particle weight and at line 30 a random number function generates random numbers ($R = FLTRNF(0)$, uniformly distributed on intervals of 0,1). Depending on the condition, it is checked first with cumulative probability for energy group, indicated by ($R - WTS(I+NWT)$) and then it is checked with the spatial distribution for mesh points of group IG (indicated by ISBIAS). The lines 50 and 55* are the weight corrections for selecting from the modified distribution which is given by the ratio of the natural probability to the biased probability at the selected energy groups.

*In this version of subroutine SOURCE, only the value of WTS(1) is considered, values greater than 1 are set equal to zero, So the weight correction is ignored.

The five lines after line 60 define the source parameters (ring source in this case). Statement " Call AZIRN(S,C) " is a random azimuthal angle ϕ which is uniformly distributed on the interval of $(0,2\pi)$. X and Y are the location of a random point on the ring source. Statement "call GTISO(U,V,W)" is an isotropic unit vector, where $U=\cos\theta$, $V=\cos\phi\sin\theta$, and $W=\sin\theta\sin\phi$. Angle θ is a random polar angle between 0 and π .

```
SUBROUTINE SOURCE(IG,U,V,W,X,Y,Z,WATE,MED,AG,ISOUR,ITSTR,NGPQT3,
1 DDF,ISBIAS,NMTG)
C
C IF ITSTR=0, MUST PROVIDE IG,X,Y,Z,U,V,W,WATE AND AG IF DESIRED TO BE
C DIFFERENT FROM CARD VALUES (WHICH ARE THE VALUES INPUT TO SOURCE)
C IF ITSTR=1, IG IS THE GRP NO. CAUSING FISSION, MUST PROVIDE NEW IG
C THIS VERSION OF SOURCE SELECTS INITIAL GROUP FROM THE INPUT SPEC
C
C This version of source produces an isotropic ring source; the
C Radius of the ring is "RADIUS = 3000.0 CM"
C
COMMON /USER/ DUM(9),I0,I1, IDUM(12)
COMMON WTS(1)
DATA ICALL/1/
    data radius/ 3000.0/
IF (ICALL) 10,10,5
5  ICALL = 0
WRITE (I0,1000)
1000 FORMAT (' YOU ARE USING THE DEFAULT VERSION OF SOURCE WHICH SETS W
1ATE TO DDF AND PROVIDES AN ENERGY IG.')
10  IF (ISOUR)15,15,60
15  WATE=DDF
    IF (ISBIAS) 20,20,25
20  NWT = 2*NMTG
    GO TO 30
25  NWT = 3*NMTG
30  R = FLTRNF(0)
    DO 35 I=1,NGPQT3
    IF (R - WTS(I+NWT)) 40,40,35
35  CONTINUE
40  IG=I
    IF (ISBIAS) 60,60,45
45  IF (I-1) 60,50,55
50  WATE = WATE*WTS(2*NMTG+1)/WTS(3*NMTG+1)
    GO TO 60
55  WATE = WATE* (WTS(2*NMTG+I)-WTS(2*NMTG+I-1))/(WTS(3*NMTG+I)-WTS(3*N
1MTG+I-1))
60  continue
    call azirn(S, C)
    x = radius * c
    y = radius * s
    z = 140.0
    call gtiso(U, V, W)
RETURN
END
```

A1.2 INPUT DATA

A1.2.1 Input data file (for ALS)

The general input file of MORSE consists of many cards. There were many input files made for the ALS skyshine calculations. The final input data, for 10000 neutrons and a 30-cm roof is explained here. The first input card is A is a comment card and the second card B contains 13 values, as follows:

- "NSTRT = 1000" number of particle per batch.
- "NMOST = 2000" maximum no. of particles allowed in the batch (ref.6).
- "NITS = 10" no. of batches.
- "NQUIT = 1" no. of sets of NITS batches to be run without calling subroutine INPUT.
- "NGPQTN = 36" no. of neutron energy groups being analyzed.
- "NGPQTG = 0" no. of gamma-ray groups to be analyzed.
- "NMGP = 37" no. of primary particle groups for which the cross_sections are stored.
- "NMTG = 37" total no. of groups for which cross_sections are stored. (NGP+NGG)
- "NCOLTP = 0" should be set greater than zero if collision tape is desired.
- "IADIM= 0" should be greater than zero for adjoint problem.
- " MAXTIM= 240.0" maximum cpu time allowed in minute for the problem to be on the computer.
- " MEDIA= 4" no. of cross_section media; should agree with NMED on card XB.
- " MEDLAB= 0" no albedo information to be read for this value.

The next data card is the card C and requires 9 variables as follows:

- ISOUR= 0 source energy group if greater than zero.
- "NGPFS= 36" No. of groups for which the source spectrum is defined.
- "ISBIAS= 0" no source energy biasing if equal to zero.
- "NQTUSD= 0" an unused variable.
- "WTSTRT= 1.0" weight assigned to each source particle.
- "EBQTN= 1.0E-5" lower energy limit of lowest neutron group in eV.
- "EBOTG= 1.0E+4" lower energy limit of lowest gamma-ray group in eV.
- "TCUT= 1.0" age in second at which particles are retired.
- "VELTH= 2.2E+5" velocity of the thermal neutron in cm/sec.

The next data card is card D which contains 7 variables as follows:

- "XSTR, YSTR, ZSTR, 0, 0, 0" coordinates for source particles.
- "AGSTR- 0.0" starting age for source particles.
- "UINP, VINP, WINP, 0.0, 0.0, 0.0" source particle direction cosines. Zero values are indicating isotropic.
- The next input card is card F. On card F the neutron energy groups are entered. For ALS skyshine problem, the neutron energies have been collapsed into 37 groups, starting with the highest energy of 1.964E+7 eV to the lowest energy of 4.140E-1 eV. These data depending on number of the energy groups can be obtained from Oak Ridge National Laboratory (NDEF library).
- card H- RANDOM "9DAD5D4CBB42" this variable is the "seed".

Card "I" has seven input variables as follows:

- "NSPLT=0" Performs splitting if set > 0 (this option was not used in any of the runs made).
- "NKILL=0" russian roulette is allowed if set > 0 (not used).
- "NPAST=0" Exponential transform is invoked if set > 0 (subroutine DIREC required for this option. Not Used).
- "NOLEAK=0" Non-leakage invoked if set > 0 (not used).
- "IEBIAS=0" Energy biasing is allowed if set > 0 (not used).
- "MXREG = 9" Number of regions described by the geometry.
- "MAXGP = 36" Last energy group on which above functions are performed.

The card "L" contains four variables as follows:

- "NSOUR = 0" Used for a fixed source problem, otherwise the source is from the fissions generated in the previous batch.
- "MFISTP = 0" Used for fission problems, for values of "0" no fission allowed.
- "NKCALC = 0" Number of first batch to be included in K calculation, for the value of "0" no estimate of K is made.
- "NORMF = 0" For the value of "0", standard weights are used, otherwise fission weights are multiplied by the latest estimate of "K" at the end of each batch.

Cards "CGA, CGB, and CGC" are the geometry and zone specifications which are explained in the "picture" section. The next card "CGD" is used to input the total number of the zones, defined on card "CGC". Card "CGE" is used to specify the material for each zone, the numbers refer to as:

- "1" is put in for the zone made with *air*.
- "2" is put in for the zone made with *concrete*.
- "0" is put in for the zone made with *vacuum*.

MORSE cross_sections are entered by the use of cards **XA-XF**, the inputs are as follows:

- Card **XA** is the title card for the cross_section. This title is presented on the output, so a definite title is imperative.

Card **XB** contains 13 variables as follows:

- "NGP=37" The total number of primary groups for which cross-sections are stored. It should be the same as "NMGP".
- "NDS=37" The number of primary downscatters for "NGP".
- "NGG=0" number of secondary group for which the cross_section are stored.
- "NDSG=0" Number of secondary downscatters for "NGG".
- "INGP=58" Total number of groups for which the cross_sections are entered.*
- "ITBL=61" Table length.*
- "ISGG=4" Location of within-group scattering cross-section (no. of upscatters + 3).
- "NMED=4" Number of media for which cross_section are to be stored. For media are entered (air, concrete, polypb, and lead). But only two sets of cross-sections for air and concrete are used.

*For computation of "INGP" refer to reference 6, table 4.1.

*reference 6, table 4.1

- "NELEM=9" Number of elements for which cross_sections are to be read. The elements are listed on card XF.
- "NMIX=11" Number of mixing operations to be performed (elements times density operations).
- "NCOEF=4" Number of coefficients for each element, including P_0 .
- "NSCT=2" Number of discrete angles.
- "ISTAT=1" Flag to store Legendre coefficient, if > 0 .

Card XC, are related to cross_sections printing. There are 11 variables on this card. All the values for the ALS are selected as zero.

Card XD, is the element identifier for the cross-section tape. Due to the use of P_3 Legendre expansion of the cross-sections 4 values for each element are picked, for example: 2, 3, 4, 5 belong to one element, and 22, 23, 24, 25, to the next element.

Card XF, is used to input the medium number and the density of each element which is used in every medium:

- KM - medium number, "1" for concrete, "2" for air, "3" for B-poly, and "4" for lead.
- KE - 1 through 9, element number occurring in medium KM (negative values indicate last mixing operation for those mediums).
- RH0 - indicates density of element KE in medium KM.

The following input cards are data read by subroutine SCORIN: 1) card AA, is only title information. 2) card BB contains the following variables:

- ND = 11 number of the detector used.
- NNE = 36 number of primary particle (neutron) energy bins to be used.
- NE = 36 total number of energy bins.
- NT = 0 number of time bins for each detector.
- NA = 0 number of angle bins.
- NRESP = ? number of energy dependent response functions to be used.
- NEX = 3 number of extra arrays of size NMTG to be set aside.
- NEXND = 3 number of extra arrays of size ND to be set aside.

Card CC, is used to enter the detector locations. It follows as X = 0.0, Y = 0.0, Z = 140.0 cm, and so on. If other than point detectors are desired, the point locations must still be input and can be combined with additional data built in to user routines to fully define each detector.

Cards FF, are the response function values. NMTG values will be read in each set of FF cards. Input order is from energy group 1 to NMTG (order of decreasing energy). Noting that all these values are for 37 neutron energy group.

The MORSE input file is formated, in the way that only five spaces are reserved for each value. Values out of the designated spaces will result in error messages.

SKYSHINE TO DETECTORS AT 244 CM HEIGHT USING 37-GROUP CROSS SECTIONS A

1000	2000	10	1	36	0	37	37	0	0.240.0	4	0	B													
				0	36	0	01.0	1.0	E-51.0	E+41.0	2.2	+5 C													
									0.0	0.0	0.0	0.0 D													
									0.0	0.0	0.0														
									0.4376E-020	0.4986E-020	0.2419E-020	0.1318E-020	0.4413E-020	0.3371E-020	0.7941E-02E1										
									0.9829E-020	0.1210E-010	0.1482E-010	0.1804E-010	0.3434E-010	0.8188E-010	0.2080E-01E1										
									0.7265E-010	0.1964E-000	0.2017E-000	0.3214E-010	0.2436E-000	0.5748E-000	0.6746E+00E1										
									0.5115E-000	0.4713E-010	0.4788E-010	0.1598E-010	0.1324E-020	0.4348E-020	0.1709E-02E1										
									0.3018E-030	0.5835E-040	0.2611E-040	0.1726E-050	0.2429E-060	0.3908E-070	0.8313E-08E1										
									0.1855E-080	0.5328E-09					E1										
									1.9640	-7	1.6805	-7	1.4919	-7	1.3840	-7	1.2840	-7	1.2214	-7 F					
									1.1052	-7	1.0000	-7	0.0484	-6	0.1973	-6	0.7408	-6	4.3763	-6 F					
									4.7237	-6	4.0457	-6	3.0119	-6	2.3852	-6	2.3069	-6	1.8269	-6 F					
									5.5023	-5	5.5764	-5	5.1109	-5	5.2475	-4	2.4788	-4	2.1875	-4	1.0333	-4 F			
									3.3546	-3	1.2341	-3	3.8295	-2	1.0130	-2	2.9023	-1	1.0677	-1	3.0590	-1 F			
									1.1254		4.140		-1												
									95AD5D4CB42																
									0	0	0	0	0	9	36										
									0	0	0	0													
									SKYSHINE IN POINT DETECTORS NEAR AHS																
									RCC	1	0.0	0.0	-100.0	0.0	0.0	0.0	344.0	CCB1							
										24500.0															
									RCC	2	0.0	0.0	0.0	0.0	0.0	0.0	244.0	CCB2							
									RCC	3	0.0	0.0	0.0	0.0	0.0	0.0	244.0	CCB3							
									RCC	4	0.0	0.0	0.0	0.0	0.0	0.0	244.0	CCB4							
									RCC	5	0.0	0.0	0.0	0.0	0.0	0.0	244.0	CCB5							
									RCC	6	0.0	0.0	0.0	0.0	0.0	0.0	244.0	CCB6							
									RCC	7	0.0	0.0	0.0	244.0	0.0	0.0	30.0	CCB7							
									RCC	8	0.0	0.0	0.0	244.0	0.0	0.0	30.0	CCB8							
									SPH	9	0.0	0.0	0.0	0.0	25000.0			CCB9							
									SPH	10	0.0	0.0	0.0	0.0	30000.0			CCB10							
									END																
									CD1	000	+1	-2						CCG1							
									AR2	0000R	+9	-1	-80R	+7				CCG2							
									WJ3	000	+4	-3						CCG3							
									W04	000	+6	-5						CCG4							
									DI5	000	+3							CCG5							
									DM6	000	+5	-4						CCG6							
									DO7	000	+2	-6						CCG7							
									WF8	000	+8	-7						CCG8							
									VD9	000	+10	-8						CCG9							
									END																
									1	2	3	4	5	6	7	8	9	CCG1							
									1	2	1	1	2	2	2	1	0	CCG11							
									DLC-31 CROSS SECTIONS FOR CON(1), AIR(2), B-POLY(3) AND PB(4)																
									37	0	0	58	61	4	4	9	11	4	2	1	KA				
									-1	0	0	0	0	0	18	0	0	0	0		XC				
									2	3	4	5	22	23	24	25	30	31	32	33	34	35	KD1		
									36	37	42	43	44	45	62	63	64	65	66	67	68	69	KD2		
									78	79	80	81	130	131	132	133							KD3		
									1	2	3	4	5	6	7	8	9								
									2	7	2.015	E-2	Conc:	81									KF1		
									3	5	4.587	E-2	Conc:	0									KF2		
									4	6	1.743	E-3	Conc:	A1									KF3		
									5	1	1.375	E-2	Conc:	B									KF4		
									6	-8	2.660	E-3	Conc:	C8									KF5		
									7	4	4.193	E-5	Air:	W									KF6		
									8	-5	1.128	E-5	Air:	O									KF7		
									9	2	6.880	E-4	B-CH2:	B									KF8		
									3	3	3.958	E-2	B-CH2:	C									KF9		
									4	-1	7.916	E-2	B-CH2:	B									KF10		
									5	-9	3.282	E-2	Lead:	Pb									KF11		
									SAMED ANALYSIS INPUT DATA									AA							
									11	36	36	0	3	3	3								BB		
									0.0	0.0	244.0														
									1P20.0	0.0	0.0	244.0													
									2000.0	0.0	0.0	244.0													
									2000.0	0.0	0.0	274.0													
									3600.0	0.0	0.0	244.0													
									5000.0	0.0	0.0	244.0													
									7000.0	0.0	0.0	244.0													
									9000.0	0.0	0.0	244.0													
									12500.0	0.0	0.0	244.0													
									17500.0	0.0	0.0	244.0													
									20000.0	0.0	0.0	244.0													
									BANK1(1,5): DOSE EQUIVALENT PER BEAM ENERGY LOST (rads/mJ)																
									4.27	+4	4.21	-4	4.21	+4	4.21	+4	4.15	+4	4.15	+4	4.15	+4	FT		
									4.15	+4	4.08	-4	4.08	+4	4.08	+4	4.08	+4	4.08	+4	4.08	+4	FT		
									4.08	+4	4.03	-4	4.00	+4	3.97	+4	3.86	+4	3.86	+4	3.86	+4	FT		
									3.50	+4	7.12	-3	4.96	+3	2.78	+3	1.85	+3	1.72	+3	0.92	+2	FT		
									9.92	+2	9.92	-2	9.92	+2	9.92	+2	9.92	+2	9.92	+2	9.92	+2	FT		
									9.92	+2	9.92	+2													
									BANK1(1,5): FLUENICES IN ELEVEN POINT DETECTORS (neuts cm-2 neut-1)																
									3.0	1.0	1.0	1.0	1.0	1.0	1.0	1.0	1.0	1.0	1.0	1.0	1.0	FT			
									3.0	1.0	1.0	1.0	1.0	1.0	1.0	1.0	1.0	1.0	1.0	1.0	1.0	FT			
									3.0	1.0	1.0	1.0	1.0	1.0	1.0	1.0	1.0	1.0	1.0	1.0	1.0	FT			
									3.0	1.0	1.0	1.0	1.0	1.0	1.0	1.0	1.0	1.0	1.0	1.0	1.0	FT			
									3.0</td																

A1.2.2 GEOMETRY

Combinatorial geometry (CG) is the basis of MORSE geometry. Every system must be described by combinations of the following geometric bodies:

- a) right parallelepiped,
- b) sphere,
- c) right circular cylinder
- d) right elliptic cylinder
- e) ellipsoid
- f) right cone (truncated or not)
- g) right angle wedge,
- h) arbitrary polyhedron of many sides
- i) circular torus

Each of these bodies may be arbitrarily oriented in space. All of the data for the geometry are put in on the card CGA in the data file (information regarding the data file will be explained later each body uses one card).

In order to define a body, a series of parameters are used for every different body. Table 5 lists, all the bodies which can be used in combinatorial geometry package with the necessary parameters to define each.

Bodies are combined into volumes called **zones** by three operators:

- a) combination of bodies using an "OR" operator
- b) exclusion of bodies using a minus "-" operator, and
- c) overlap of bodies using a plus "+" operator

The geometry of the Advanced Light Source is produced by combining 8 right circular cylinders and two surrounding spheres (the dimensions and input data are explained in the data file section). Figure A.1 shows the description of body types that was used to

Table 5. MORSE input data for different bodies.

Card Column	TYPE	IALP 1-5	IALP 7-10	Real Data 11-20	Real Data 21-30	Real Data 31-40	Defining 41-50	Particular Body 51-60	61-70	Number of Cards Needed
Box	B ₀ X	IALP is assigned by the user or by the	V _x H ₂ X X _{min} code if left	V _y H ₂ Y X _{max} V _x	V _z H ₂ Z Y _{min} V _y	H ₁ X H ₃ X Y _{max} R	H ₁ Y H ₃ Y Z _{min} -	H ₁ Z H ₃ Z Z _{max} -	1 of 2 2 of 2 1	
Right Parallel- Piped	R _P P	by the user or by the	X _{min} -	X _{max} -	Y _{min} -	Y _{max} -	Y _{min} -	Y _{max} -	1 of 2 2 of 2	
Sphere	S ₀ M		V _x V _y V _z	V _x V _y V _z	V _x V _y V _z	R	-	-	1	
Right Circular Cylinder	R _C C	blank.	V _x R	V _y R ₁ Y	V _z R ₁ Z	H ₁ X R ₂ X	H ₁ Y R ₂ Y	H ₁ Z R ₂ Z	1 of 2 2 of 2	
Right Elliptic Cylinder	R _E C		V _x R ₁ X	V _y R ₁ Y	V _z R ₁ Z	H ₁ X R ₂ X	H ₁ Y R ₂ Y	H ₁ Z R ₂ Z	1 of 2 2 of 2	
Ellipsoid	E ₀ L		V ₁ X L	V ₁ Y -	V ₁ Z -	V ₂ X -	V ₂ Y -	V ₂ Z -	1 of 2	
Truncated Right Cone	T _R C		V _x L ₁	V _y L ₂	V _z -	H ₁ X -	H ₁ Y -	H ₁ Z -	1 of 2 2 of 2	
Right Angle Wedge	W _E or R _A W		V _x H ₂ X	V _y H ₂ Y	V _z H ₂ Z	H ₁ X H ₃ X	H ₁ Y H ₃ Y	H ₁ Z H ₃ Z	1 of 2 2 of 2	
Arbitrary Polyhedron	A _R H		V ₁ X V ₃ X V ₅ X V ₇ X	V ₁ Y V ₃ Y V ₅ Y V ₇ Y	V ₁ Z V ₃ Z V ₅ Z V ₇ Z	V ₂ X V ₄ X V ₆ X V ₈ X	V ₂ Y V ₄ Y V ₆ Y V ₈ Y	V ₂ Z V ₄ Z V ₆ Z V ₈ Z	1 of 5 2 of 5 3 of 5 4 of 5	
Face Descriptions (see note below)										5 of 5

Termination of
Body Input Data END

form the ALS geometry and explained as follows:

1) Right Circular cylinder (RCC): first a common vertex V at the center of one base is specified, a height H is expressed in the terms of its X, Y, Z components, and a scalar R denoting the radius.

2) Sphere(SPH): on the common vertex V a radius R denoting the sphere radius.

More complete geometry data for more bodies is listed in reference 6 (table 4.3 page 00052).

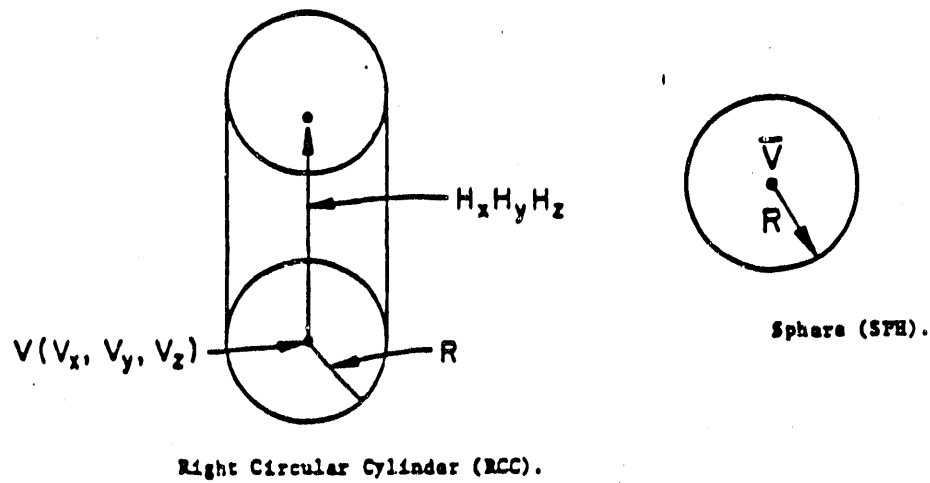


Figure A.1, Coordinates for a right circular cylinder and a sphere as used in MORSE input.

PICTURE

The picture program is created to help a user to determine if the intended geometry has been used. PICTURE displays, as printed output, two dimensional slices through the specified geometry. A regularly spaced array of points generated and each point is plotted as a number related to either media, or zone depending on the option selected. The executive routine for the picture program reads the input data, calculates the coordinates of the picture to be plotted and controls the calls to other routines. Figure A.2 is the input image of the ALS picture run, the input image consists of several input cards as following:

```
0 0 TEST: SKYSHINE FOR ALS
RCC 1 0.0 0.0 -100.0 0.0 0.0 344.0 CGA
      24500.0
RCC 2 0.0 0.0 0.0 0.0 0.0 244.0 CGB1
      24500.0
RCC 3 0.0 0.0 0.0 0.0 0.0 244.0 CGB2
      2680.0
RCC 4 0.0 0.0 0.0 0.0 0.0 244.0 CGB3
      2725.0
RCC 5 0.0 0.0 0.0 0.0 0.0 244.0 CGB4
      3150.0
RCC 6 0.0 0.0 0.0 0.0 0.0 244.0 CGB5
      3196.0
RCC 7 0.0 0.0 244.0 0.0 0.0 30.0 CGB6
      2680.0
RCC 8 0.0 0.0 244.0 0.0 0.0 30.0 CGB7
      3196.0
SPH 9 0.0 0.0 0.0 25000.0 0.0 0.0 CGB8
SPH 10 0.0 0.0 0.0 30000.0 0.0 0.0 CGB9
END CGB10
GD1 000 +1 -2
AR2 0000R +9 -1 -80R +7 CGC1
WI3 000 +4 -3 CGC2
WO4 000 +6 -5 CGC3
DI5 000 +3 -4 CGC4
DM6 000 +5 -6 CGC5
DO7 000 +2 -7 CGC6
RF8 000 +8 -9 CGC7
VD9 000 +10 -9 CGC8
END CGC9
1 2 3 4 5 6 7 8 9 CGD1
0 1 0 0 1 1 0 0 CGE1
0 0 GEOMETRY FOR LIGHT SOURCE SKYSHINE: ZONES
0.0 0.0 300. 6000. 0.0 -200. PC
0.0 0.0 -1.0 1.0 0.0 0.0 PD
100 120 10.0 50. PE
0 1 GEOMETRY FOR LIGHT SOURCE SKYSHINE: MATERIALS
0.0 0.0 300. 6000. 0.0 -200. PC
0.0 0.0 -1.0 1.0 0.0 0.0 PD
100 120 10.0 50. PE
0 1 FF
```

Figure A.2, Input image of ALS picture.(with 30-cm thick roof)

1. cards CGB1 to CGB10, body parameters are input from a common vertex.
2. cards CGC1 to CGC9, is used to combine bodies to make zones.
3. card PA assigns numbers to different zones and bodies (character or alphabets could be used as well). 9 numbers for 9 zones.
4. card PB (References 1 and 6)
5. card PC has two variables :

INCT= 0 or 1

0 means after this picture, return to PC for another picture with the same geometry.

1 means after this picture, read in a new geometry.

6. IRG= -1, 0, 1

-1 means, display the region geometry.

0 displays the zone geometry

1 displays the material geometry.

7. card PD: the first three X, Y, Z, coordinates of the upper left corner in the combinatorial geometry. the second three number are the X, Y, Z, of the lower corner of the picture.

8. card PE: the first three digit are the direction numbers proportional to the direction cosines for the U axis of the picture. U point down toward the page. The second three numbers are direction numbers for V axis. The V axis points to right across the page.

9. card PF sets the format: NU number of intervals to print along the U axis. NV number of intervals to print along the V axis.

DELU spacing of intervals along the U axis.

DELV spacing of intervals along the V axis.

Figure A.3 is the output display of a cross-section of the geometry of the Advance Light Source by program PICTURE. The dotted region is concrete and the region marked by 1's is air.

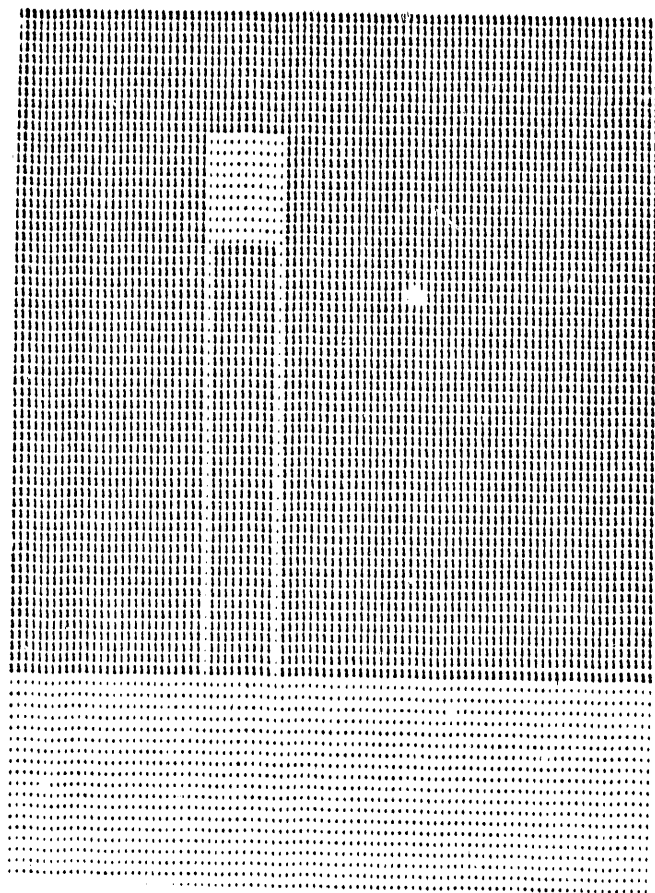


Figure A.3, Output of program picture.

A1.2.3 Fluence to dose conversion by ICRP factors.

The fluence to dose conversion factors were obtained as follows:

first, an average energy \bar{E} is computed as a simple average of upper and lower energy of each of 36 energy group, then from \bar{E} and graph of figure A.4. the ratio of dose to flux is obtained. MORSE computes the total dose-equivalent by the following equation:

$$H = \sum_{i=1st}^{36th} \Phi_i \Delta E_i \left(\frac{H_i}{\phi} \right) \quad (A.1)$$

Φ_i , is the fluence computed by MORSE in, $n/(cm^2 \cdot eV \cdot n)$. Table 6 contains other energy values used to compute the dose-equivalent.

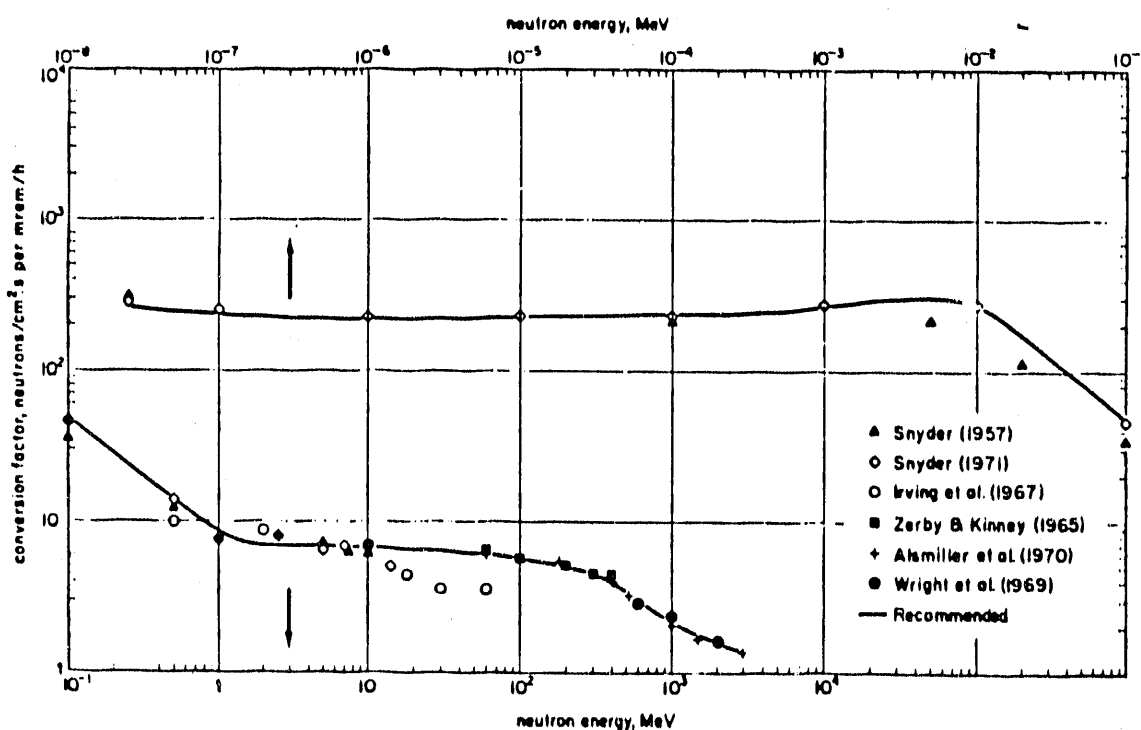


Figure A.4, Conversion factors for neutron. The curves indicate the values recommended by the commission.

Table 6 Energy data for fluence to dose-equivalent conversion.

Energy Group	Energy Range(MeV)	ΔE (MeV)	\bar{E} (MeV)	$\frac{H}{\phi}$ (*)
1	19.64-16.91	2.74	18.3	4.27
2	16.91-14.92	1.99	15.9	4.27
3	14.92-14.19	0.73	14.6	4.27
4	14.19-13.84	0.35	14.0	4.27
5	13.84-12.84	1.00	13.3	4.27
6	12.84-12.21	0.63	12.5	4.27
7	12.21-11.05	1.16	11.6	4.27
8	11.05-10.00	1.05	10.5	4.27
9	10.00-9.05	0.95	9.5	3.97
10	9.05-8.19	0.86	8.6	3.97
11	8.19-7.41	0.88	7.8	3.97
12	7.41-6.38	1.03	6.9	3.97
13	6.38-4.97	1.41	5.7	3.97
14	4.97-4.72	2.42	4.8	3.97
15	4.72-4.07	0.66	4.4	3.97
16	4.07-3.01	1.05	3.5	3.97
17	3.01-2.39	0.627	2.7	3.97
18	2.39-2.31	0.078	2.4	3.97
19	2.31-1.83	0.480	2.1	3.97
20	1.83-1.11	0.719	1.5	3.47
21	1.11-0.55	0.558	0.83	2.31
22	0.55-0.16	0.393	0.35	1.54
23	0.16-0.11	0.0047	0.15	.794
24	0.11-0.053	0.057	0.082	.471

Energy Group	Energy Range(MeV)	ΔE (MeV)	\bar{E} (MeV)	$\frac{H}{\phi}$ (*)
25	53,000-25,000	28,000	39,000	.242
26	25,000-22,000	3,000	24,000	.185
27	22,000-10,300	11,700	16,150	.116
28	10,300-3,355	6,945	6,827	.093
29	3,355-1,234	2,121	2,295	.093
30	1,234-583	651	908	.099
31	583-101	482	342	.116
32	101-29	72	65	.116
33	29-10.7	18.3	19.9	.116
34	10.7-3.1	7.6	6.9	.126
35	3.1-1.13	1.97	2.12	.126
36	1.13-.414	.716	.772	.126

(*) $\frac{H}{\phi}$ is in mrem/(n/cm⁻²) $\times 10^{-5}$

A2.0 TOTAL POWER RADIATED PER ELECTRON

Power radiated for acceleration is:

$$P(t) = \frac{2}{3} \frac{e^2}{c^3} \frac{\gamma^2}{m^2} \left(\frac{dp}{dt} \right)^2 \quad (A.2)$$

where

$$\frac{dp}{dt} = \omega \times p^2 = \frac{V}{R_m} \times m \gamma V \quad (A.3)$$

is the magnitude of the rate of change of momentum for circular motion, and for $V \approx c$, the radiated power for one magnetic section is:

$$P = \frac{2}{3} \frac{e^2}{R_m^2} c \gamma^4 \quad (A.4)$$

The energy radiated by a magnetic section is,

$$E = P \times t \quad (A.5)$$

where $t = 2\pi \frac{R}{c}$. Noting that the particle radiates when it goes around the bending magnet

($R \approx R_m$), The total energy is given ($E = E_{tot}$):

$$E_{tot} = \frac{4\pi}{3} \frac{e^2 \gamma^4}{R_m} \quad (A.6)$$

Then the total power per e^- is obtained by $P_{tot} = E_{tot} / t$:

$$P_{tot} = \frac{2}{3} \frac{e^2}{R_m R} c \gamma^4 \quad (2.3)$$

A3.0 BREMSSTRAHLUNG

Equation 2.5 is based on the parameters corresponding to an existing electron storage ring very close to the ALS parameters (the electron ring is constructed at the physical science laboratory of the university of Wisconsin at Madison). The target vacuum pipe is made of stainless-steel with a maximum energy of 1 GeV and with 288 Jules of stored energy.

The unshielded bremsstrahlung dose in the plane of the ring source, is given as a function of a distance r_i (fig. A.5) from the ring. The circumference of the ring has been divided into 1° intervals. The dose at the point P is computed by obtaining the angle θ_B between the beam and tangent to the point of beam loss. Assuming a uniform beam loss around the beam, the dose at every interval is computed by:

$$W_i = \frac{W}{360}$$

The total dose at P is

$$\sum_{i=1}^{i=360} \frac{D(\theta_B, W_i)}{r_i^2}$$

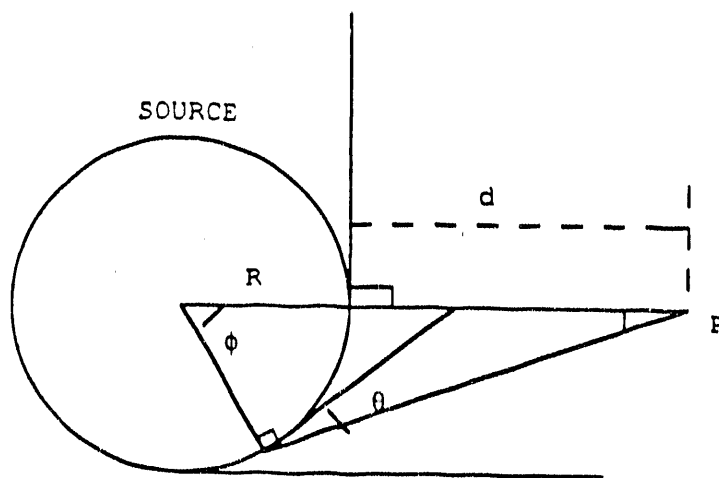


Figure A.5. Geometry for bremsstrahlung dose calculations at point P. A distance d from the beam.

$$D(\theta_B, W_i) = (6 \times 10^4 E^2)^{-\frac{(\theta_B)}{\theta_{14}}} \cdot 3 \times 10^6 \times 10^{-\frac{(\theta_B)}{21}} \cdot 9 \times 10^4 \times 10^{-\frac{(\theta_B)}{110}} \cdot \frac{1}{3.6 \times 10^6} \quad (2.5)$$

$$r_i^2 = R^2 + (R+d)^2 - 2R(R+d)\cos\phi_i \quad (A.7)$$

The bremsstrahlung angle is obtained by the following equation:

$$\theta_{B_i} = \cos^{-1} \frac{(R+d)\sin\phi_i}{r_i} \quad (A.8)$$

A4.0 Sources of radiation for shielding calculations

From equation 3.1, the source is given as:

$$Y' = (1.21 \times 10^8 Z^{0.66} n/J)(1000 J/fill) \left(\frac{1}{3.3 \times 10^{12} \text{ fill}/e} \right) \left(\frac{E}{1.9 \text{ GeV}} \right)$$

This will result the following relation:

$$Y' = 1.9 \times 10^{-2} E Z^{0.66} n/e \cdot \text{GeV}$$

From reference 18, equation 5, the source is:

$$Y = 1.49 \times 10^{-2} E Z^{0.73} n/e \cdot \text{GeV}$$

With $Z = 26$ (stainless steel), comparison of $Y = 1.60 \times 10^{-1} E$, and $Y' = 1.63 \times 10^{-1} E$ shows the accuracy of the source data. With $Y' = 3.7 \times 10^{-2} n/e^-$ and a flux to dose conversion factor of $3.5 \times 10^{-8} \text{ mrem.cm}^2/\text{n}$, the source will yield:

$$Y' = \frac{1.2 \times 10^{-9} Z^{0.66} E}{4\pi(1.9)} \text{ rem.cm}^2/e^-$$

then the total neutron giant resonance obtained by Fig. A.6 is:

$$DE(GR) = 5.0 \times 10^{-11} E \left(\frac{\cos \theta}{a+d} \right)^2 Z^{0.66} \exp \left(\frac{-d \rho \sec \theta}{\lambda_2} \right) \text{ rem}/e^- \quad (\text{A.9})$$

Equation A.9, compares to equation 6a of reference 3.

high energy neutrons (HEN).

Above the neutron energy 100 MeV The neutron dose equivalent is given by the following equation:(Ref. 3)

$$DE(HEN) = 1.73 \times 10^{-11} E_o (\cos \theta)^2 \frac{\exp \left(\frac{-d \rho \sec \theta}{\lambda_1} \right)}{(1-0.72 \cos \theta)^2 (a+d)^2} \text{ Rem}/e^- \quad (\text{A.10})$$

λ_1 removal mean-free path for neutrons, for concrete = 120 g/cm^2 . because of the inelastic cross-section it is constant above 100 MeV.

The maximum dose equivalent for high energy neutron, happens directly above the source and at some angle as a function of shield thickness. The maximum dose can be shifted toward 90° angle as shield thickness is increased (fig. 8, Ref. 3).

photons.

Dose from the energy electrons are given as :

$$DE(\text{photon}) = \frac{1.78 \times 10^{-9}}{(1-\cos\theta)^{1.2}} E_0 \left(\frac{\cos\theta}{a+d} \right)^2 B \exp\left(\frac{-\mu}{\rho} d \rho \sec\theta\right) \text{Rem/e}^- \quad (\text{A.11})$$

So the total dose equivalent is summarized into the following equation:

$$D.E(\text{total}) = D.E(\text{HEN}) + D.E(\text{GR}) + D.E(\text{photons})$$

$\frac{\mu}{\rho}$ mass attenuation coefficient which because the energy is carried by photon with energies at compton is assumed constant. Assuming 8 MeV photons, this values for concrete is $0.024 \text{ cm}^2/\text{g}$.

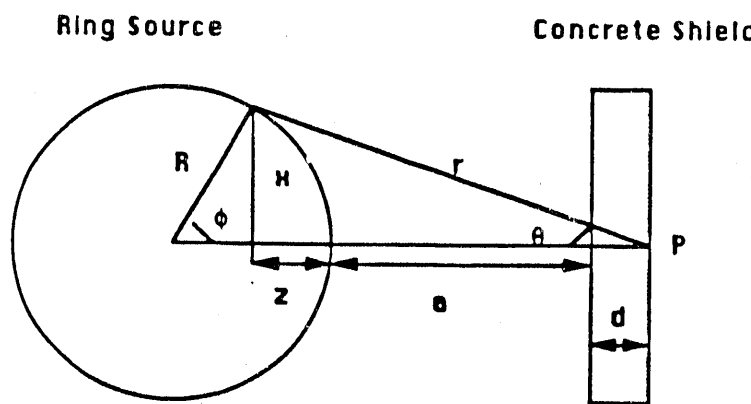


Figure A.6, Assumption for giant resonance equation 7.1.

END

DATE FILMED

01/10/91

